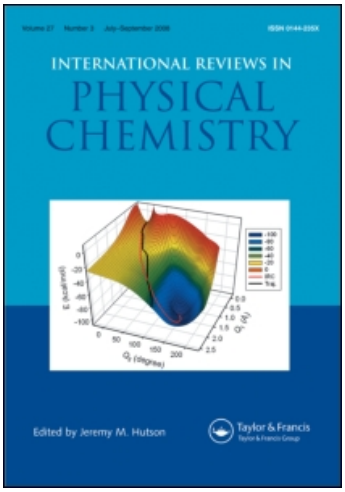

International Reviews in Physical Chemistry
Publication details, including instructions for authors and subscription information:
http://www.informaworld.com/smpp/title~content=t713724383

Chiral discrimination in the confined environment of biological nanospace: reactions and interactions involving amino acids and peptides

Nilashis Nandi[a]
[a] Chemistry Department, University of Kalyani, Kalyani, Nadia, West Bengal 741235, India

To cite this Article Nandi, Nilashis(2009) 'Chiral discrimination in the confined environment of biological nanospace: reactions and interactions involving amino acids and peptides', International Reviews in Physical Chemistry, 28: 2, 111 — 167
To link to this Article: DOI: 10.1080/01442350902999682
URL: http://dx.doi.org/10.1080/01442350902999682

International Reviews in Physical Chemistry
Vol. 28, No. 2, April–June 2009, 111–167

Taylor & Francis
Taylor & Francis Group

Chiral discrimination in the confined environment of biological nanospace: reactions and interactions involving amino acids and peptides

Nilashis Nandi*

Chemistry Department, University of Kalyani, Kalyani, Nadia, West Bengal 741235, India

(*Received 15 March 2009; final version received 22 April 2009*)

Although chiral discrimination in biological systems is overwhelmingly present, its molecular mechanism remained a puzzle. Why the basic blocks of life like L-amino acid and D-sugar are not being scrambled and retain enantiomeric purity since evolution is an unresolved question. In the present review we focus on the recent experimental and computational studies on the chiral discrimination in reactions such as peptide synthesis and aminoacylation. Experimental studies have shown that a clear homochiral preference exists favouring L-amino acid. Recent combined quantum mechanical/molecular mechanical studies explain the high level of stereospecificity of the processes and revealed multiple factors responsible for the discrimination and concomitant retention of the biological homochirality. Chirality of the relevant molecular segments and the intricate interaction between them as well as with the surrounding residues are important. The confinement of the chiral reactants within the biological nanospaces like the peptidyl transferase centre in tRNA and active site of the aminoacyl transferase as well as the nanoscale proximity are important for the manifestation of the discrimination. Multiple favourable influences of the stereochemistry of the natural chirality (D-form) of the sugar ring are noted. This explains the heterochiral relationship of the D-sugar and L-amino acid in biology. In addition to factors such as chirality, confinement and nanoscale proximity of the molecular segments, the network of electrostatic interaction present in the active site plays a significant role in the chiral discrimination in aminoacylation. Chiral discriminations in the biological cavities of nucleic acid and cyclodextrin are also briefly reviewed.

Keywords: chiral; discrimination; nanospace; ribosome; peptide; aminoacylation

Contents

*Email: nilashisnandi@yahoo.com

ISSN 0144–235X print/ISSN 1366–591X online

DOI: 10.1080/01442350902999682
http://www.informaworld.com

1. Introduction

Chirality is omnipresent in biological, biomimetic and non-biological material systems. Traditionally, a lack of symmetry is considered to be the signature of chirality. This broad definition includes diverse macroscopic objects such as hands, animal organs, biological organisms, and macromolecules, mesoscopic objects such as small to medium sized aggregates of molecules as well as microscopic objects such as molecules as chiral entities where the absence of symmetry elements can be noted. A molecule possessing an asymmetrically substituted carbon atom may be chiral. However, chiral molecules without asymmetric carbon atoms exist and instances of achiral molecules with more than one asymmetric carbon atoms are well known. More generally, the molecules which lack axis of improper rotation (also known as alternating axis of symmetry or rotation-reflection axis) should be considered as chiral and are dissymmetric. As improper rotations are regular rotations followed by a reflection in the plane perpendicular to the axis of rotation, a necessary and sufficient condition for the chirality of a molecule is that it cannot be superimposed on its mirror image. Such a dissymmetric molecule may or may not have a simple axis of symmetry while both symmetry elements are absent in an asymmetric molecule [1,2]. The decisive influence of chirality (dissymmetry) can be observed at all levels of the structural hierarchy of biological systems, starting from the primary level to the higher levels (secondary and tertiary) of their architecture. A vast majority of these systems exhibit a preference for one specific chiral form of the constituent molecular structure over the corresponding mirror image. Nature is specific regarding the chirality of amino acids and proteins, sugars and RNA or DNA. A strong homochiral preference for L-amino acid and D-sugar at the primary level and a heterochiral relationship between these two specific isomers from a pool of isomers was fixed early in the evolutionary history [3] in building up the proteins and nucleic acids using these fundamental building blocks of life. This is a signature of the preference of one chiral form over the other (chiral discrimination).

Chiral discrimination is used in the literature as a rather broad term encompassing various properties of the chiral systems. For example, in theoretical and computational studies, the differences between the absolute energies of L- and D- isomers (a small energy difference) [4,5] as well as the differences between intermolecular energies of enantiomeric (L–L) and racemic (D–L) pairs as a function of separation (a small but non-negligible energy

difference as a function of distance and a significant energy difference as a function of mutual orientation) [6–9] are used as the measures of chiral discrimination. In experimental studies, various macroscopic, mesoscopic or microscopic length scale observables are also used to study the chiral discrimination phenomena [9]. Examples are the major differences in the isotherm features of a Langmuir monolayer composed of pure enantiomeric (L–L or D–D) or racemic (D–L) monolayers, significantly different shapes or handedness of enantiomeric or racemic monolayer domains or bilayer aggregates in the condensed phase and the differences in the lattice structures of the enantiomeric or racemic monolayers, respectively. The origin of chiral discrimination is, in general, difficult to comprehend because the formation energies (enthalpies and Gibbs free energies) and most properties (except those depending on chirality) are identical for the two enantiomers. Consequently, it is equally baffling to follow the molecular reasoning of the discrimination of the systems composed of enantiomeric and racemic molecules. From a molecular perspective, chiral discrimination is a phenomenon where it is possible to distinguish the intermolecular interaction of the identical molecules of a homochiral nature (either R–R or S–S) with the interaction between the molecule and its mirror image (racemic type; R–S) or a different chiral molecule. The manifestation of this difference could be diverse, expressed as observables at macroscopic, mesoscopic and microscopic length scales in biological, biomimetic and material systems.

A schematic description of the chiral discriminations observed at various length scales in a few common biological, biomimetic and non-biological systems are shown in Figure 1. The length scales mentioned in the diagram should be considered as approximate only since sharp boundaries do not exist for micro-, meso- or macro-length scales. For example, the overall sizes of the condensed phase monolayer domains often range in micrometre length scale. Chiral discrimination can be noted in biological systems as L-amino acid and D-sugar are preferred over the corresponding enantiomers. Preference of chirality of lipids is also noted, which belongs to biomimetic systems. Various material systems exhibit chiral discrimination at microscopic length scale. Chiral discrimination is noted in transition of metal-catalysed stereospecific polymers [10], diverse helical polymers [11], polymers composed of polysaccharides and their derivatives [12], polysilanes [13] and various other polymeric materials [14]. The chiral discrimination noted in these systems is observed at the microscopic length scale of $\sim$0.5–1 nm as well as in mesoscopic length scale in the range of $\sim$1–10 nm (for larger polymers). Examples of discrimination in mesoscopic length scale in biological systems are abundant. Most common examples are the helices, β-sheets and chiral domains composed of these subunits [15]. Amphiphilic aggregates in bilayers [16–18, and references therein] and monolayers [9,19–22] form aggregates with curved dissymmetric shapes in three dimensions and two dimensions, respectively, and are examples of mesoscopic biomimetic systems exhibiting chiral discrimination. Chiral discrimination is also exhibited by liquid crystalline systems [23]. It is to be noted that, for such structures, the borderline between mesoscopic and macroscopic is not to be considered as rigorous since the domains or aggregates can be larger depending on the number of subunits or number of molecules in aggregate. The quaternary structure of proteins [24,25], RNA or DNA helical structures or their supercoiled structures, large dissymmetric polymers or even biological organs are examples of a macroscopic chiral object where discrimination is observed. It is important to point out that in the present review we principally refer to the phenomenon of chiral discrimination where electromagnetic interaction has a

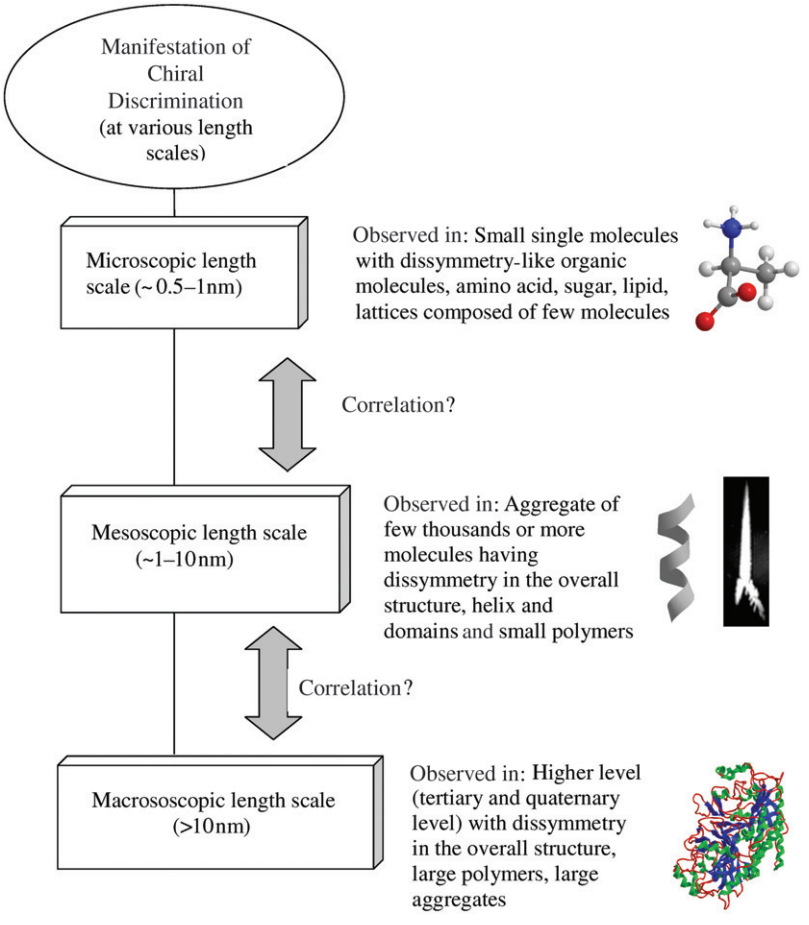

Figure 1. [Colour online] Schematic diagram showing the chiral discrimination observed at various length scales. The length scales mentioned in the diagram should be considered as approximate only as no rigorous boundaries exist for micro-, meso- or macro-length scales. For example, the domains formed in monolayers are often sized as several micrometre. As mentioned in Section 1, the diagram principally refers to the chiral discrimination in systems where electromagnetic interaction has dominant contribution in the discrimination. Hence, the discriminations arising from chiralities noted at the level of sub-atomic particles ($<10^{-5}$ nm) and at the cosmic length scale are beyond the scope of this review and are not mentioned in the diagram.

dominant contribution. Hence, the discriminations arising from chiralities noted at the level of sub-atomic particles (less than $\sim 10^{-5}$ nm) and at the cosmic length scale are beyond the scope of this review [26–28].

As chiral discrimination is expressed by diverse systems including biological, biomimetic and non-biological systems, the questions concerning the discriminations are many. A few such questions are mentioned in Figure 2. Of course, the questions pertaining to the chirality effects are not limited to those mentioned in the figure and so many other questions can be asked. However, the following questions are relevant in relation to the

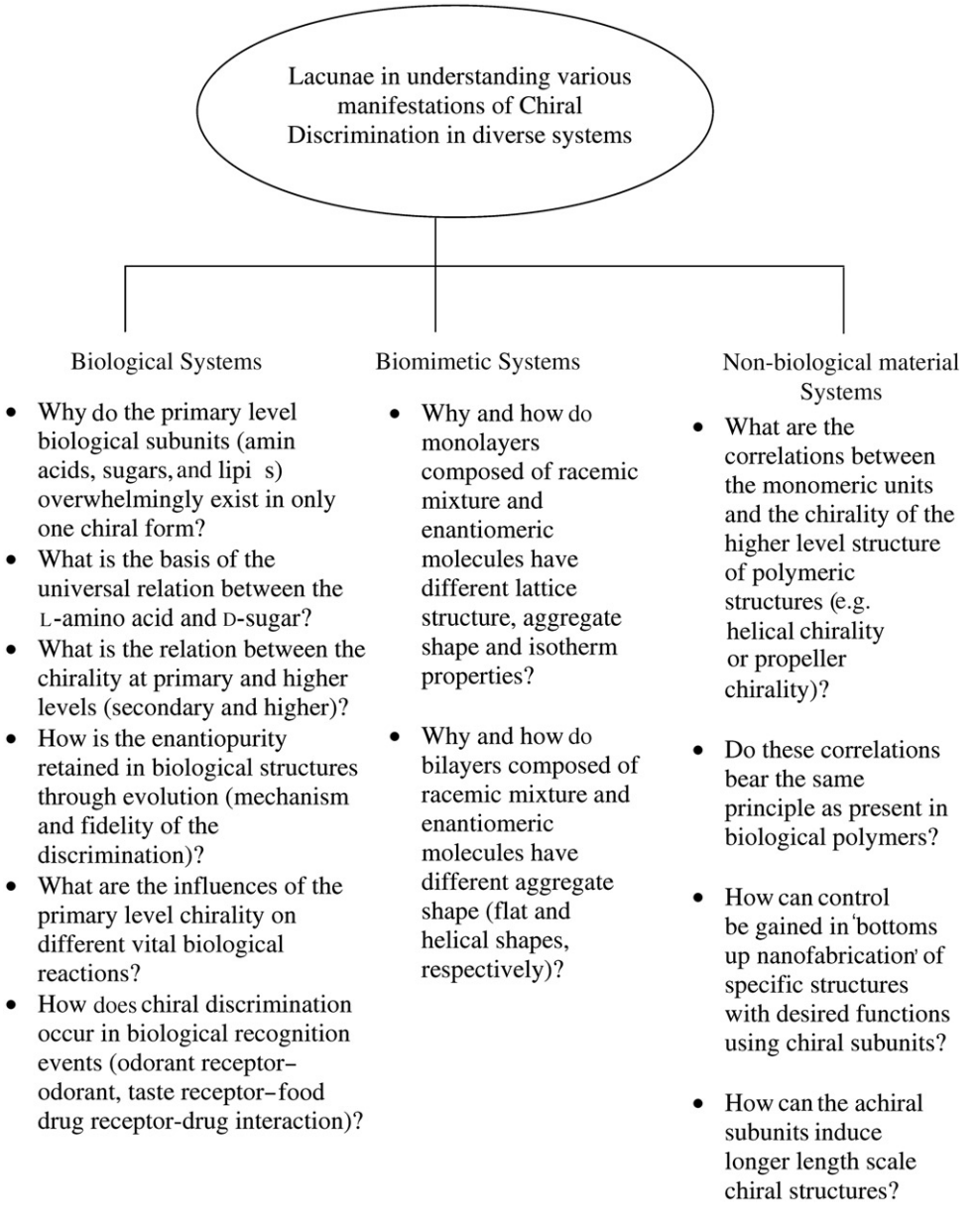

Figure 2. Schematic diagram showing few questions pertaining to the chiral discrimination observed in biological, biomimetic and non-biological material systems.

experimental and computational studies on chiral discrimination in biological systems in recent years. Due to the obvious importance of the understanding of evolution and life processes, the origin of the specific chirality of biological structures remains a subject of continued interest [29–31]. Another question is why the primary level biological subunits (amino acids, sugars and lipids) overwhelmingly exist in only one chiral form?

A related question is how nature utilises these chiral structures present at various length scales of biological systems for different functions and what are the mechanisms of doing so? Explicitly one can ask what is the basis of the universal relation in nature that is as observed between the L-form of amino acid and D-form of sugar in composing RNA or DNA and protein structures. The answer to this question shall address the mutual relation between the realms of protein and that of the nucleic acid. The genetic process, which includes coding and protein synthesis, is specific about the structural relationship between amino acids and sugars in nucleotides. A complementary relation couples amino acid and nucleotides at both monomeric and polymeric level. Heteropairing of amino acid (L-enantiomer) and sugar (D-enantiomer) in today's living world is of the greatest preference by evolution. The preferred heteropairing of the L-amino acid and D-sugar over the other pairing possibilities indicates a biological chiral discrimination. The preference for other heteropairs (D-amino acid and L-sugar) and homopairs (either L-sugar: L-amino acid or D-sugar: D-amino acid) seems unlikely and is out-competed by the natural heteropair. The specificity of the chiral heterocoupling of the enantiomeric forms of amino acids and sugars in functional biological systems indicates that the origin could be in the structure–function relationship of the heteropair. This specificity might have originated through the prebiotic evolution and retained thereafter. On the other hand, amino acids and sugars can racemise in aqueous medium, which could be a part of the prebiotic environment. This poses a problem in understanding the development of the enantiomeric excess of sugar and amino acids in D- and L-form, respectively, as well as the retention of the same, which are important problems to investigate. Considering the fact that racemisation is a common event in chemical reactions, another puzzle is how the enantiopurity is retained in biological structures through evolution (mechanism and fidelity of the discrimination). Answer to this question is related to the understanding of the problem regarding what are the influences of the primary level chirality on different vital biological reactions and how the chiral discrimination occurs in biological recognition events (e.g. odorant receptor–odorant, taste receptor–food, drug receptor–drug interaction) [32,33]? The questions, of course, do not end up at the level of the chirality of small-scale biological structure. The relation between the chirality at primary and higher levels (secondary and higher) is also an important problem to investigate, which could provide understanding about nature's principle in building up complex structures using basic subunits [34]. Related problems in biomimetic systems like monolayers and bilayers have been addressed [6,9,16–22]. Of particular interest was the question of why and how monolayers composed of racemic mixture and enantiomeric molecules have different lattice structure, aggregate shape and isotherm properties. Similarly, why and how bilayers composed of racemic mixture and enantiomeric molecules have different aggregate shape (flat and helical shapes, respectively). The answers to these questions relate to the chirality at the microscopic level and to the chirality at the mesoscopic level. The questions pertaining to the biomimetic systems have been addressed by molecular level studies (both experimental and theoretical) in recent years and the correlation between microscopic and mesoscopic chirality is now better understood for biomimetic systems [6,9,19–22]. This indicates that molecular structure has a critical influence on the higher order aggregate formed.

The answer to these foregoing questions and particularly why the basic blocks of life are not being scrambled and retain enantiomeric purity is challenging as many biological systems incorporate D-amino acids as well as racemise in other cases. In many cases, a

specific chirality (L- or D-form) is either generated or involved in molecular fragment(s) in the course of many vital biochemical reactions involving chiral amino acids, peptides and sugars. While the incorporation of D-amino acids is a hallmark of peptide synthetase-based non-ribosomal peptide synthesis [35–38] and posttranslational modification [39–41], RNA-dependent ribosomal synthesis of peptides and proteins exclusively incorporates only the 20 natural amino acids and selenocysteine with their natural chirality (L-form). Incorporation of D-amino acids to an organism can be toxic if it does not naturally occur in the same [42–52]. On the other hand, D-amino acid naturally occurs in selected systems like peptidoglycans of bacterial cell walls (D-Ala- and D-Glu-), peptide antibiotics [42,53–56] and in the human brain (D-Asp and D-Ser are present at high concentrations) [57–61]. Transformation of L-enantiomer by a racemase can also lead to the development of D-enantiomer. Conversion of the L- to the D-stereoisomer of tryptophan was observed in the presence of tryptophan synthetase [62,63]. The D-tyrosine might arise at the step of the addition of an amino group to 4-hydroxyphenylpyruvate [64]. Moreover, D-amino acids are likely to be non-specifically formed as side reaction products in the presence of pyridoxal phosphate-containing enzymes or of pyridoxal phosphate alone [65,66]. The presence and development of D-enantiomers in some specific organisms only and exclusion of it in the natural biosynthetic pathway of protein synthesis in today's world raise the question about the mechanism of discrimination. On the other hand, the racemic compound in crystalline state being more stable than enantiomeric form, it is a question of how the chances of racemisation throughout the course of evolution till today are avoided [67].

Molecular understanding of the chiral discrimination recently emerged in the case of biomimetic systems [19–22]. The discrimination arises from the fact that the atom(s) or group(s) attached to the chiral centres of D and L enantiomers exchange the position in space which results in the change of the interaction in enantiomeric and racemic pairs as a function of mutual distance and orientation. This subtle phenomenon controls the longer length scale architecture composed of chiral molecules and induces different handedness of curvature and is dependent on intermolecular interaction. The intermolecular pair potential between chiral molecules is strongly orientation dependent in the condensed phase of monolayers and the nature of the orientation dependence is different for the enantiomeric and racemic pair. The observed orientation dependence acts over a mesoscopic length scale in the condensed phase, where the rotational degrees of freedom are restricted due to the dense packing of neighbouring molecules relative to the fluid monolayer phase. The favoured mutual orientation drives the neighbouring enantiomeric molecules in the condensed state progressively arranged in a specific handedness and controls the features of the higher level chiral structure (helices in the case of a bilayer and curved domains in the case of a monolayer). Such specific orientation dependence is absent in the corresponding racemic state and no helicity or curvature is noted there. Confinement of the molecules at the proximity of nanometre length scale is an important factor in the expression of the chiral discrimination at the mesoscopic length scale. At such nanoscale separation, the intermolecular energy profile has specific orientation-dependent minima, which is absent at larger separation. The discrimination reduces at larger intermolecular separation in the case of monolayer domains. When the molecules are widely separated, the molecules can have many degrees of freedom and the dissymmetric nature of the orientation-dependent interaction is averaged out. No preferential mutual

orientation is observed in the molecular aggregate and manifestation of chiral discrimination vanishes. This is observed in the liquid-expanded and gaseous phases of the monolayer [19–22]. The same trend is noted in the case of a bilayer where the helicity is observed at lower temperatures [16,17]. In summary, a few factors are noted to be important for discrimination to be significant in biomimetic systems. The chirality of the molecules makes the intermolecular interaction profile dissymmetric and orientation-dependent. The energetically favoured mutual orientation is the controlling factor of the morphology in the condensed phase of aggregates. Confinement by the surrounding molecules within a range of few nanometres is also important for successful discrimination. The confinement enhances the population of molecular arrangement with a preferred orientation rather than arbitrary mutual orientation between molecules for an ensemble of molecular orientational states.

Natural biological systems developed by evolution are arguably the best to carry out the discrimination. In the course of the dynamics of a biological system, the reacting molecular segments in the active-site approach within the proximity of nanodimension. This is a state of reduced degree of freedom for the corresponding segments compared to the free state of the same in the bulk and this reduction in rotation and translation might enhance the stereoselectivity. The influence of the chirality of molecules on the orientation-dependent intermolecular interaction and the effect of the confinement seem to dictate the chiral discrimination in biological systems also. It is long recognised that the enzymes, which are inherently chiral, are needed to orient both substrates and catalytic residues to preferentially stabilise one stereoisomeric transition state over another in the enzymatic reactions. The effectiveness of the catalytic activity of an enzyme in the rate enhancement significantly depends on the realisation of tight binding, which is coupled with a high degree of steric recognition [68,69]. Proper orientation between the substrate and the catalytic residue is a necessary prerequisite for effective binding in the restriction of degrees of freedom. The restriction of degrees of freedom is also another important factor in steric recognition. It is long known that diffusion in reduced dimension can speed up biological interaction over the limits normally set by three-dimensional diffusion processes [70]. The fidelity of generation of L-configuration of the amino acid by transamination reaction is dependent on the addition of a proton to a particular face of the quinonoid intermediate and the confinement and effective orientation plays a role. Successful mimics of catalytic enantioselective transamination fixes the reactants in optimal geometry to enhance the reactivity [71]. A number of other examples are known similar to the transamination reaction, where the confinement within the nanodimension of the active site is important for the stereoselectivity. For the racemisation and epimerisation at the active sites of epimerase and racemase, it is necessary that the corresponding enzyme needs to clamp down on the substrate and should have been placed in a proximal relative position [72]. Consequently, the confinement of the chiral moieties in a nanoscale separation is important for chiral discrimination.

The focus of the present review is on a few questions asked in biological systems (shown in Figure 2), particularly, (1) on the influence of the amino acids and sugars (primary level structures) on some vital biological reactions, (2) on the mutual influence of L-amino acid and D-sugar in these life processes, (3) retention of enantiopurity in these processes (mechanism and fidelity of the discrimination) and (4) the effect of the confinement in the nanometre length scale within the active site on the discrimination

exhibited by the reaction. Since these life processes are the one in which enantiopurity is retained through evolution, they are ideal to address the questions asked. If the mechanism of discrimination can be answered, that might also provide a clue to the question of why the primary level biological subunits (amino acids, sugars and lipids) overwhelmingly exist in only one chiral form.

Among the life processes, there are cases where the chiral discrimination is known to be vital and significant. Peptide synthesis in the ribosomal peptidyl transferase centre (PTC) is a tremendously important process, which takes place in the ribosome. Ribosome is a multifunctional molecular machine in all living cells that performs protein synthesis by sequentially reading out the genetic code as message from mRNA chain and concomitantly translates the corresponding amino acid sequence [73,74]. The major substrates of this vital reaction are chiral (amino acid segments present in the peptidyl tRNA and aminoacyl tRNA, bound to the ribosome at P- and A-site, respectively, and the sugar rings of the nucleic acid structure). Each of these moieties is confined within a proximity of the nanometre length scale. Since the PTC contains both amino acid and sugar, the reaction is also suitable to address the question of the heterochiral relationship of the D-sugar and L-amino acid. In relation to the question of why a chiral amino acid would prefer a specific enantiomeric form of the sugar (Figure 2) it might be noted that a few possible factors are important to explore. It is suggested that one chiral building block like an amino acid might induce asymmetry in other building block such as a sugar [75]. Another suggestion is that an environment, which could help concentrate either L-amino acid or D-sugar (or both), could help til evolution in the specific chiral direction [76]. A related question – how the specificity of the natural heteropair in biochemical reactions related to life processes is retained till date – is also unanswered. It is possible that an environment, which is favourable for either L-amino acid or D-sugar (or both), could help retain the chiral preference. It is tempting to assume that the biological cavity like PTC, in which confined chiral amino acids or sugars undergo functional reaction, may provide impetus for such chiral discrimination. If the interaction of the confined amino acid or sugar (or both) undergoing the related biochemical reactions exhibits chiral discrimination, then the related reaction in the concerned biological cavity (e.g., PTC in ribosome) could help in discriminating the amino acid or sugar of preferred chirality. With this end in view we first present the review of the literature on experimental and computational studies on chiral discrimination in the peptide synthesis in the PTC in the Section 1 and 2, respectively.

Another biological reaction, which is a necessary prerequisite of the peptide bond formation, is the aminoacylation reaction in aminoacyl tRNA synthetase (AARS). The reaction involves chiral subunits like amino acids and sugars and the AARSs are designed by evolution to carry out discrimination in an extremely efficient way. The AARSs specifically incorporates a particular amino acid and ensures that only cognate substrates are selected from the large cellular pool of similar amino acids or tRNA. This process involves an acylation site and may contain an editing site. The reaction also involves chiral reactants (e.g. amino acids, sugar ring or acetylates) which have restricted degrees of freedom within the active site and are confined in a nanodimension. Experimental and computational studies on chiral discrimination in the aminoacylation reaction in the active site of the aminoacyl transferase are reviewed in Sections 3 and 4, respectively. Finally, in Section 5, chiral discrimination in the interactions involving amino acids and peptides in

biological cavities of nucleic acid, cyclodextrin are reviewed where the chiral selectivity is found to be important.

2. Chiral discrimination in the peptide synthesis in the ribosomal PTC: experimental studies

Out of the several partial reactions of protein biosynthesis, peptidyl transferase reaction is one of the most intensively studied. In this reaction, the nucleophilic α-amino group of the aminoacyl tRNA attacks the electrophilic carbonyl carbon of the ester bond linking the peptide moiety to the P-site tRNA carrying an aminolysis of the ester bond. This is shown in Figure 3. The reaction occurs in the ribosome, which is a large complex (~2.5 MDa in bacteria) and consists of two subunits (small subunit, 30S and large subunit, 50S). Although the ribosome is made up of RNA and proteins, the PTC where the reaction happens is essentially composed of nucleic acid with no protein present within 1.5 nm distance of the active site. A model of PTC with A- and P-terminals is shown in Figure 4. As mentioned in Section 1, the chiral discrimination in peptide synthesis in PTC can arise from the interaction between the two terminals and the surrounding bases and nearby D-sugar rings in the RNA structure. Several pieces of evidence suggest that the accuracy in chiral discrimination in ribosomal peptide synthesis is controlled by the chiral amino acid terminals, chiral sugar rings involved and structure of the PTC including the achiral bases.

In the present section, we focus on the results of the studies on discrimination in peptide synthesis. In many cases the incorporation of D-amino acid by aminoacylation (a prerequisite for the formation of aminoacyl-tRNA) is difficult or even impossible in many cases. As the D-amino acid could not be incorporated as a reacting terminal in the tRNA or its analogue, the synthesis of D–L peptide could not be performed in such cases. This is a problem in studying the discrimination. Thus, various results concerning the reaction are obtained not only based on tRNA but also using different analogues in the *in vitro* experiments. The substrate specificity of the peptide synthesis process, especially as

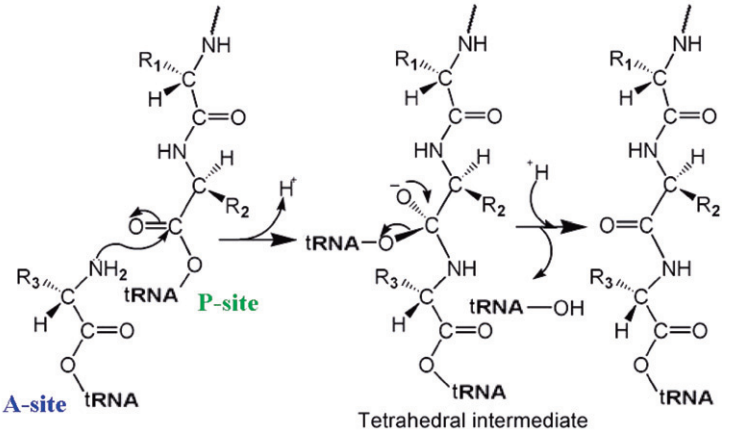

Figure 3. [Colour online] Scheme of the peptide bond formation at the PTC in ribosome (reprinted from reference [97] with permission from the American Chemical Society. © American Chemical Society).

regards to the structural nature and spatial orientation of the aminoacyl moiety, has been investigated using analogues of puromycin, aminoacylated nucleotides structurally related to the 3′ terminus of tRNA [77–79] and tRNA analogues in which the cognate amino acid was maintained in a 'defined' spatial orientation [80–82]. The intermolecular interaction will be influenced by the different relative spatial arrangements of the reacting moieties, different degrees of proximity and confinement with neighbouring residues in such different systems and the resulting discrimination is expected to be different. Hence, various experimental results on chiral discrimination in peptide synthesis must be interpreted keeping in mind the corresponding states of the reacting amino acid segments

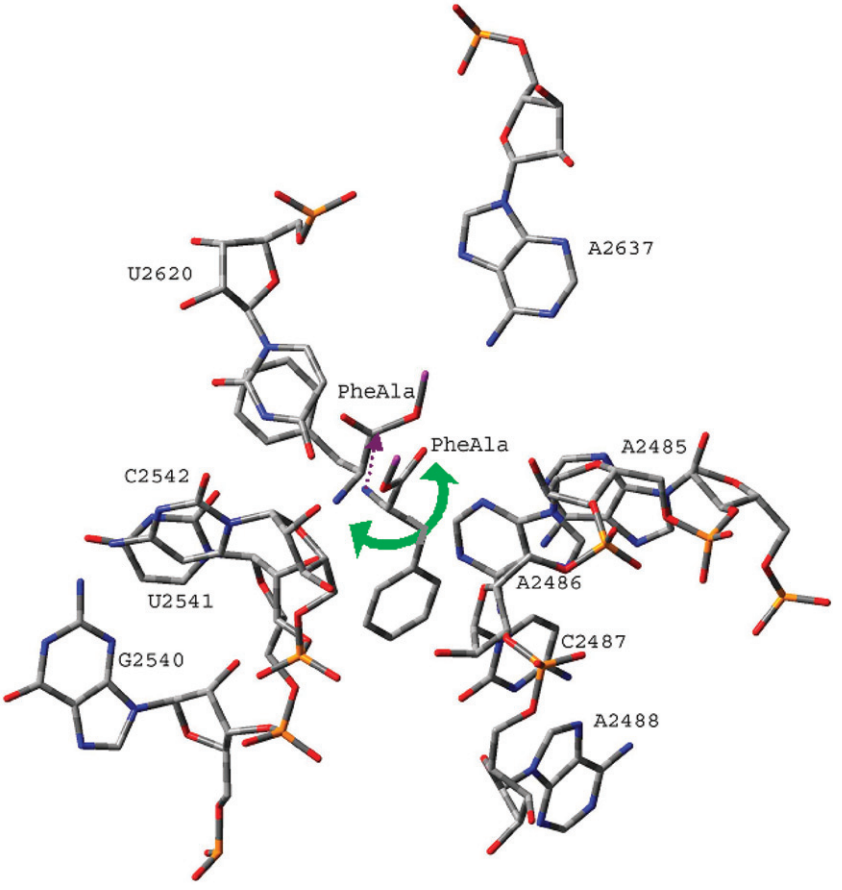

Figure 4. [Colour online] A model of the PTC based on the crystal structure of CCA-Phe-cap-biotin bound simultaneously at half-occupancy to both the A-site and the P-site of the 50S ribosomal subunit. The segments are taken from the crystal structure of the ribosomal part of *Haloarcula marismortui*. (PDB ID: 1Q86 [80]). Residues include (all numbering corresponds to scheme as in *Haloarcula marismortui*): A76 of CCA attached to phenylalanine at A-terminal, A76 of CCA attached to phenylalanine at P-terminal, A2485, A2486, C2487, A2488, U2620, A2637, G2540, U2451 and C2452. (reprinted from reference [99] with permission from the American Chemical Society. © American Chemical Society).

(their degrees of freedom, proximity and orientation with each other and interaction with surrounding residues).

In an earlier study, Calender and Berg [83] observed that D-tyrosine could be esterified to $tRNA^{Tyr}$ and then could be incorporated into peptides. D-Tyrosine was incorporated into the peptide in an assay for a protein synthesising system containing *Escherichia coli* ribosome, a supernatant fraction of *Bacillus subtilis* (in which the D-tyrosyl RNA is stable) and poly-UA (as messenger). The L-tyrosine incorporation is 114 μmoles and D-tyrosine incorporation is only 19 μmoles. The reduced (about one-sixth of L-isomer) incorporation of D-tyrosine indicates that the protein synthetic system is unfavourable towards the incorporation of D-amino acids into peptides and is an example of homochiral preference in the peptide synthesis process.

Yamane *et al.* [84] studied stereoselectivity of the aminoacyl tRNA binding to the A-site and peptide bond formation. Overall rate of dipeptide formation is 30-fold higher for L-isomer compared to the D-isomer. It is noted that 75–90% of D-Tyr-tRNA dissociates from the ribosome while <30% of L-Tyr-tRNA is lost through this pathway. Their estimate is that 6-fold rate difference arises in binding of tRNA to the A-site and 5-fold rate difference arises in the peptide formation. This is another example of strong discrimination favouring homochiral synthesis.

In a series of pioneering studies, Hecht and co-workers studied in detail the achievability of incorporation of D-amino acid into ribosome. Misacylated tRNAs like *N*-acetyl-D-phenylalanyl-$tRNA^{Phe}$, *N*-acetyl-L-tyrosyl-$tRNA^{Phe}$, *N*-acetyl-D-tyrosyl-$tRNA^{Phe}$ and *N*-acetyl-β-phenylalanyl-$tRNA^{Phe}$ were used to study the P-site binding and peptide bond formation in a cell free system involving *E. coli* ribosome programmed with poly-uridylic acid [85,86]. Unlike the $tRNA^{Phe}$s activated with L-phenylalanine and L-tyrosine, the *N*-acetyl-D-phenylalanyl-$tRNA^{Phe}$ and *N*-acetyl-D-tyrosyl-$tRNA^{Phe}$ performed poorly for dipeptide formation when L-phenyl alanyl-$tRNA^{phe}$ acts as acceptor (A-site) tRNA. However, it could not be established that this inability is due to the poor binding of these tRNAs with the ribosomal P-site or due to their inefficiency to participate in the peptide synthesis reaction. Another study confirms the foregoing results [87]. The relative yield of dipeptide synthesis for D-analogue is only 7% and 13% for *N*-acetyl-D-tyrosyl-$tRNA^{Phe}$ relative to the L-*N*-acetyl phenylalanyl-$tRNA^{Phe}$. The small amount of dipeptide produced indicates that the D-isomer incorporation is severely inhibited compared to the natural isomer [85]. Further influence of the chiral structure of the amino acid moiety is noted for *N*-acetyl D, L β-phenylalanyl-$tRNA^{Phe}$. The relative yield of dipeptide synthesis for the analogue is 110–130% relative to the L-*N*-acetyl phenylalanyl-$tRNA^{Phe}$. The authors indicated that the normal position of the *N*-acetyl amino group on C^{α} is not optimal for the peptide bond formation. Modification of the chiral structure can enhance the efficacy of the reaction. The studies by Hecht and co-workers confirm the earlier studies of Calendar and Berg as well as that of Yamane and Hopfield that the incorporation of D-amino acids into a peptide is unfavourable relative to the incorporation of natural enantiomer. It is also pointed out that structural modification leads to better performance of the reaction.

In order to understand the structural requirements for the participation as an acceptor in the reaction, Roesser *et al.* [88] have developed an approach for the preparation of aminoacyl-tRNA analogues bearing non-cognate aminoacyl moieties. A number of pyroglutamylaminoacyl-tRNAs are prepared by T4 RNA ligase-mediated condensation of

synthetic pyroglutamylaminoacyl-pCpAs with tRNAs from which the last two nucleotides at the 3′-end had been removed. The derived pyroglutamylaminoacyl-tRNAs were incubated in the presence of calf liver pyroglutamate aminopeptidase, which effected their conversion to free aminoacyl-tRNAs. The lack of contaminating esterase activities in the pyroglutamate aminopeptidase was verified by direct assay for the presence of the aminoacyl moieties in the formed aminoacyl-tRNAs and by the use of the deblocked aminoacyl-tRNAs as acceptors in the peptidyltransferase reaction using an *E. coli* ribosomal system. Different misacylated *E. coli* $tRNA^{Phe}$s prepared by T4 RNA ligase-mediated chemical aminoacylation are treated with pyroglutamate aminopeptidase. Putative deblocked L-phenylalanyl-$tRNA^{Phe}$ prepared by this procedure participated as an acceptor in the peptidyltransferase reaction fully as well as the authentic aminoacyl-tRNA. Two $tRNA^{Phe}$s bearing non-cognate amino acids (*N*-pyroglutamyl-L-O-methyl-tyrosyl-$tRNA^{Phe}$and *N*-pyroglutamyl-L-phenylglycyl-$tRNA^{Phe}$) are also able to participate as acceptors in the peptidyltransferase reaction following enzymatic deblocking. This observation verifies both the ability of pyroglutamate aminopeptidase to act as a substrate and the ability of the formed aminoacyl-tRNAs to participate in peptide bond formation. In contrast, neither *N*-pyroglutamyl-D-phenylalanyl-$tRNA^{Phe}$ nor *N*-pyroglutamyl-D-tyrosyl-$tRNA^{Phe}$ acted as an acceptor in the peptidyltransferase reaction following treatment with pyroglutamate aminopeptidase, and *N*-pyroglutamyl-D, L-β-phenylalanyl-$tRNA^{Phe}$ produced dipeptide only to the extent of 8%. The finding that the putative D-aminoacyl-$tRNA^{Phe}$s failed to act as acceptors in the peptidyl-transferase reaction parallels earlier studies.

The results of the diminished activity of D-isomer as noted by Hecht and co-workers are corroborated by the works of Bain *et al*. [89]. In an alternative approach, in the presence of nonsense codons incorporated in mRNA (codons that effect termination of peptide synthesis as there is no corresponding tRNAs) like 5′UAG, 5′UAA and 5′UGA, a compensatory DNA mutation can lead to the production of mutated tRNA (called suppressor tRNA) after activation with a normal amino acid. The presence of the suppressor tRNA during *in vitro* cell-free translation of mRNA containing a nonsense suppression site can incorporate non-natural amino acids. While, tRNAs activated with iodotyrosine, *N*-methylphenylalanine or glycine functioned well in suppression but D-pheylalanyl-tRNA did not. The result that D-amino acid fails to get incorporated is reproduced by both a normal rapid assay method as well as by the direct analysis of the isolated HPLC fraction.

The significant influence of the chirality of the sugar ring involved in the CCA moiety is also noted [90]. This result is very important in understanding the heterochiral relationship of D-sugar and L-amino acid in peptide synthesis, where the former is present as a part of the tRNA structure. While, the *N*-acetyl-D-phenylalanyl-$tRNA^{Phe}$ and *N*-acetyl-D-tyrosyl-$tRNA^{Phe}$ produced only a small amount of dipeptide, the 2′ and 3′ deoxyadenosine analogues (L-*N*-acetyl phenylalanyl-$tRNA^{Phe}$-CC2′dA and L-*N*-acetyl phenylalanyl-$tRNA^{Phe}$-CC3′dA) produced no detectable dipeptide formation. The result indicates that the effect of the sugar ring chirality is decisive over the peptide bond formation and alteration of the chirality of the same is unfavourable for the synthesis. Suppression efficiencies of misacylated D-phenylalanyl-$tRNA^{Gly}_{CUA}$-dCA is nil as compared to other misacylated phenylalanyl-$tRNA^{Gly}_{CUA}$-dCA.

The discrimination is also studied in different model systems. Puromycine is a small molecule mimic of aminoacyl-tRNA (aa-tRNA) and acts as a universal translation inhibitor by entering the ribosomal A-site and participating in the peptide bond formation with the nascent peptidyl chain. The structure of puromycine is shown in Figure 5. Puromycin blocks protein synthesis by acting as an analogue of the charged RNA after aminoacyl-RNA formation. It substitutes for an incoming aminoacyl-RNA as the acceptor of the carboxyl-activated peptide and forms peptidyl-puromycin. While peptidyl-tRNA in ribosome is normally transferred to the amino group of the next aminoacyl-tRNA, the carboxyl-activated peptide is transferred to puromycin. This causes ending of

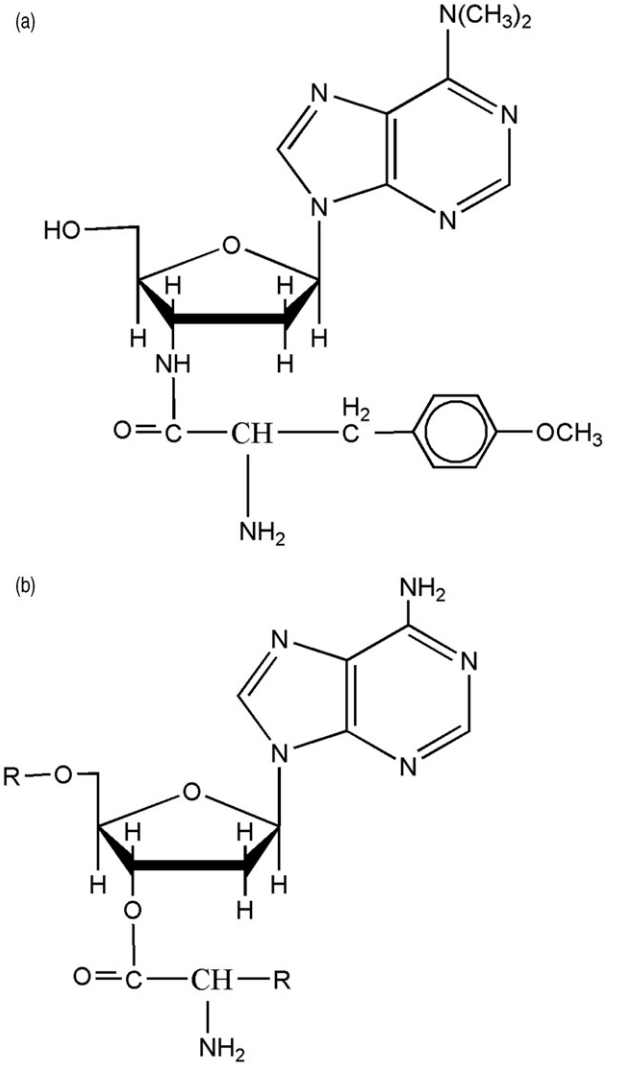

Figure 5. The chemical structure of (a) puromycin [91] and (b) model of the aminoacyl part of the tRNA.

the sequential extension of peptide and stops the growth of the nascent peptide chain [91]. Note that the orientational degrees of freedom of A- and P-terminals in such analogues are in principle different from those of a tRNA in the active site. Hence the discrimination might be different in these two cases.

Starck *et al*. [92] used a series of synthetic puromycin analogues to measure the activity of D-amino acid and β-amino acids in an intact eukaryotic translation system (rabbit reticulocyte ribosome). Thus, the puromycin derivatives differ in amino acid stereochemistry and amino acid moiety as well as the number of carbon units in the amino acid backbone. The activity of the model compounds is measured in a high dynamic range IC_{50} potency assay using the rabbit reticulocyte protein synthesis system. While the L-puromycin [9-{3′-deoxy-3′-[(4-methoxy-L-phenylalanyl)amino]-β-D-ribofuranosyl}-6(N,N′-dimethylamino)purine] inhibits globin mRNA translation with an IC_{50} value of 1.8 μm, the corresponding D-isomer (D-puromycin or 9-{3′-deoxy-3′-[(4-methoxy-D-phenylalanyl)amino]-β-D-ribofuranosyl}-6(N,N′-dimethylamino)purine) inhibits globin translation giving an IC_{50} value of 280 μm. The difference is 150-fold. The activity of a modified puromycin derivative (9-{3′-deoxy-3′-[(4-methyl-L-phenylalanyl)amino]-β-D-ribofuranosyl}-6(N,N′-dimethylamino)purine or L-(4-Me)-Phe-PANS) is found to be highest, giving an IC_{50} value of 1.0 μm. However, its D-amino acid isomer has an IC_{50} value of 2400 μm; even lower than D-puromycin and 2400-fold less potent than the corresponding L-isomer. Alanine analogues show little difference (~3-fold) between the L- and D-isomer. The size and geometry of the side chain is suggested to play an important role in the synthesis with larger hydrophobic side chains having improved function. It is also indicated that the structural basis of the stereoselectivity could not be addressed due to the unavailability of the high resolution structure of the rabbit reticulocyte ribosome. However, modelling of the placement of D-puromycin in the active site of *Haloarcula marismortui* 50S subunit is attempted for which the high resolution structure is available. U2620 residue is found to be the closest nucleotide to the D-side chain. This view is supported by the structural analysis suggesting that the steric hindrance of the molecular segments of D-amino acid could lead to unfavourable incorporation of D-isomer [93]. The role of the surrounding environment of the active site and particularly the role of U2620 in the discrimination in the peptide synthesis has been recently studied using computational methods and will be further discussed in the following section.

The foregoing studies indicate that attempts to incorporate D-amino acids into proteins using chemically misacylated suppressor tRNAs in cell-free protein synthesising systems were unsuccessful. Dedkova *et al*. [94] pointed out that alteration of the peptidyltransferase centre might lead to enhanced D-amino acid incorporation. Mutations in the 23S rRNA in the region of PTC and helix 89 leads to conformational change in the ribosome that alters its behaviour in the protein synthesis. Modified ribosomes with mutations in regions 2447–2450 (belongs to PTC region) and 2457–2462 (belongs to helix 89 region) of *E. coli* 23S rRNA and cell-free protein synthesising systems were prepared from mutant ribosomes. These systems were analysed for their ability to incorporate D-Met and D-Phe into protein *in vitro* in terms of UAG codon suppression. A high level of suppression in the presence of D-methionine (23%) and D-phenylalanine (12%) is observed. This indicates that in ribosome, active-site structure is, at least partly, responsible for the discriminating mechanism against D-aminoacyl-$tRNA_{CUA}$s in the ribosomal A-site. Putative alterations may lead to enhanced incorporation of D-amino acid. The result indicates that the

surrounding of the PTC has a major influence on the process of synthesis. This result is supported by recent computational studies where it is shown that the removal of a residue can reduce the chiral discrimination and will be discussed in the following section.

While it is virtually impossible to incorporate D-amino acid into proteins without modifying the chemical structure of the PTC of naturally occurring tRNA, it is possible to perform the corresponding D–L peptide bond formation in the model puromycin system. It may be noted that the alignment and surrounding environment of the amino terminals in the two cases are different. The attachment of the amino acid moieties at the CCA end of amino and peptidyl terminals restricts their free rotation. The limited available orientational degrees of freedom are, however, different in the different systems studied: tRNA or puromycin or other analogues as pointed out before. Consequently, the degrees of freedom available and the extent of confinement do vary, which affects the interaction and discrimination in these cases.

3. Chiral discrimination in the peptide synthesis in the PTC: computational studies

The experimental results in the previous section show that the chiral discrimination in peptide synthesis is significant and the incorporation of D-amino acid is unfavoured in natural synthesis. However, the understanding of the molecular mechanism of the discrimination was unavailable until recently. Also, the theoretical studies on chiral discrimination in small models as well as biomimetic systems revealed that the effect of nanoscale proximity of the chiral molecules and their restricted state are important for discrimination. The discrimination arises as a non-negligible energy difference as a function of distance and a significant energy difference as a function of mutual orientation between L–L and D–L pairs [9,19–22]. It is also necessary that the molecules should be present in the condensed state and at low temperatures. Theoretical studies also indicated that the discriminating nature of the profiles diminishes at large separation or higher temperature. In an earlier theoretical study, Salem and co-workers concluded that the discrimination is small at freely rotating limit and only six body or higher order interactions will give rise to non-zero value for the relative difference between the two virial coefficients of L–L and D–L pairs (considered as a chiral discrimination parameter) at the infinite temperature [95]. This result is also supported by subsequent theoretical studies [7,8]. A detailed classical Monte Carlo simulation using Lennard-Jones and electrostatic terms (CHARMM force field) is performed to compute the chiral discrimination between the two enantiomers of alanine (in a continuum of relative dielectric permittivity to mimic water) by Andelman and Orland [8]. The discrimination is found to slightly favour homochirality and mainly comes from the steric hindrance at short distances. However, not only the distance dependence of intermolecular interaction but also the orientation dependence of the same has a decisive role in the chiral discrimination of mesoscopic aggregates of biomimetic amphiphiles and peptides [6,22,34].

Crystallographic studies on peptide synthesis have established that a rotatory motion leads to orientation dependence of the interaction energy of the A-terminal with the P-terminal during the peptide bond formation. If the corresponding energy profile of the L–L pairs is more favourable than the D–L pair in the span of orientations covered in the rotatory motion then the difference could be a factor influencing discrimination. In the absence of any surrounding residue, the discrimination is expected to appear solely from

the non-bonded interaction between the amino acid residues themselves and not from the influence of the surrounding moieties of the nanospace. Structural analysis suggested that either the steric hindrance of the molecular segments of D-amino acid or improper orientation for the nucleophilic attack by the amino group could lead to unfavourable incorporation of D-isomer [92,93]. The significant influence of the chirality of the sugar ring attached to the CCA moiety is also noted [90]. All these possible influences on discrimination has been recently examined in a series of studies as described below.

Peptide bond formation is studied using *ab initio* methods for L-alanine dipeptide formation considering both concerted and stepwise mechanism [96]. In this study, the reacting amino acids are not covalently linked to any part of a larger structure as they are linked when present in the CCA terminal in tRNA during peptide synthesis in PTC and not surrounded by the active-site residues. It is unlikely that chiral discrimination will be exhibited in such a system as the reacting moieties are free to assume various mutual arrangements without being constrained as they are not covalently linked to a larger structure (RNA) and neighbouring residues (part of the PTC). As a result, discrimination is not expected to be observed, which is averaged out over all possible mutual orientations. However, in tRNA, the reacting segments in PTC are constrained as they are covalently linked with A- and P-terminals and located in the proximity of nanometer range. The A- and P-terminals are surrounded by nucleic acid residues, which are also within nanoscale separation. Consequently, the reaction in the PTC satisfies all the criteria necessary for significant and observable discrimination as noted in biomimetic systems. Thus, it is not surprising that discrimination in peptide synthesis is noted in experiment as described in the previous section.

The discrimination in the intermolecular energy surfaces of a pair of alanine molecules in the restricted orientational state (a model of state of the A- and P-site terminals in PTC) is investigated [97]. Starting from the optimised structures of the non-bonded homochiral (L–L) and heterochiral (D–L) pairs of molecules, the energy surfaces are studied with rigid geometry by varying the distance and orientation. The molecular arrangement is shown in Figure 6. The differences of the intermolecular energy surfaces of enantiomeric (L–L) and racemic (D–L) molecular pairs as a function of orientation are studied for an alanine molecule in the optimised geometry in its neutral and zwitterionic state using *ab initio* theory (HF′6-311++G**) as a function of mutual orientation Figure 7(a–f).

The plot shows that the interaction energy of L–L pair and the corresponding interaction energy of the D–L pair is not identical neither with the variation of the distance nor with the variation of the mutual orientation of two molecules. The potential energy surfaces of the L–L and D–L pairs are found to be dissimilar and reflect the underlying chirality of the homochiral pair and racemic nature of the heterochiral pair. The plot of the L–L pair is dissymmetric revealing the underlying chirality of the molecules. In contrast, the plot for the D–L pair is symmetric around 180° orientation, which reveals the racemic state of the neutral pair where the charge dissymmetry is also absent. Unlike the neutral case, the asymmetric charge distribution of the neighbouring molecules (starting geometry) breaks the symmetry of the energy profile of the D–L zwitterionic pair, which can be observed in the corresponding dissymmetric nature of the energy profile. The conformational energy differences between the D or L molecules themselves are negligibly small (the energies are identical for their optimised structures) and the observed difference in the intermolecular potential (ΔE_{LL-DL}) is not due to any conformational difference.

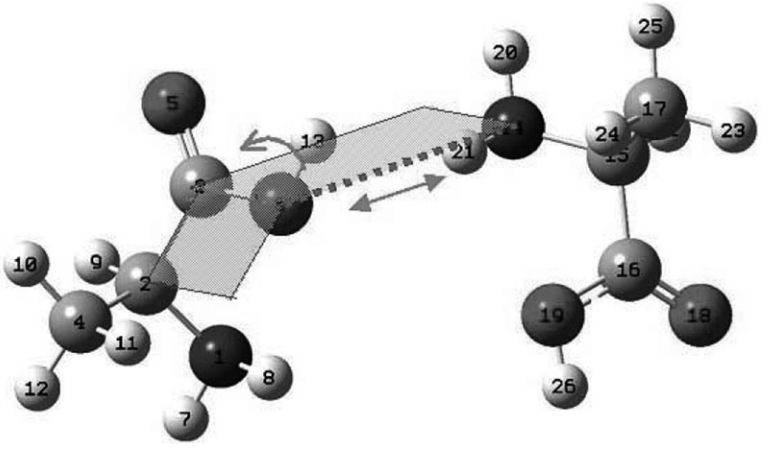

Figure 6. The scheme of mutual dihedral angle variation in a pair of non-bonded neutral L–L alanine molecules to study the discrimination in the orientation-dependent interaction (reprinted from reference [97] with permission from the American Chemical Society. © American Chemical Society).

The deviation in energies for the zwitterionic case between the L–L pair and D–L pair is due to the difference in the position of proton between the amide groups and the carboxyl group in the respective cases.

It is pointed out that the very large difference between the energy surfaces of the L–L and D–L pairs at specific orientations at the same distances between corresponding pairs is due to short-range repulsive interactions (more specifically, due to different distance dependence of the same for the L–L and the D–L pair). In general, the short-range repulsive part of both van der Waals and electrostatic (Coulombic, dipolar or multipolar) interaction varies more sharply than the corresponding long-range attractive part of the intermolecular interaction [98]. The energy profile of L–L at a given short-range separation is less unfavourable than the corresponding energy profile of the D–L pair at the same intermolecular separation. However, the energy changes over small separation distance are large at such short-range intermolecular distance and this causes the large discrimination observed. The favourable electrostatic interaction is further contributing to the large homochirality of the ΔE_{LL-DL} for the zwitterionic pair in addition to the short-range steric repulsion (which is the major source of the discrimination for neutral molecules). The basis set superposition error (BSSE) corrected results show enhanced discrimination. Use of higher-level Møller–Plesset perturbation theory (MP2) and further BSSE correction do not change the conclusions made at the Hartree–Fock (HF) level (Figure 8a and b). The major conclusions based on HF and MP2 level calculations remain unaltered when the calculations of the potential energy surfaces for the neutral and zwitterionic pairs are repeated using the B3LYP/6-311++G** level of density functional theory (DFT).

During the A-P rotatory motion, the L–L and D–L pairs of A- and P-terminals have to pass through orientations other than that intermolecular mutual orientation which corresponds to the optimised geometry of the pair of molecules (while the individual molecules may remain in their optimised geometry). This passage is easier for the L–L pair rather than for the D–L pair. In other words, during the rotatory process of A to P, the L–L pair will pass through relatively low-energy regions compared to the D–L pair. The study

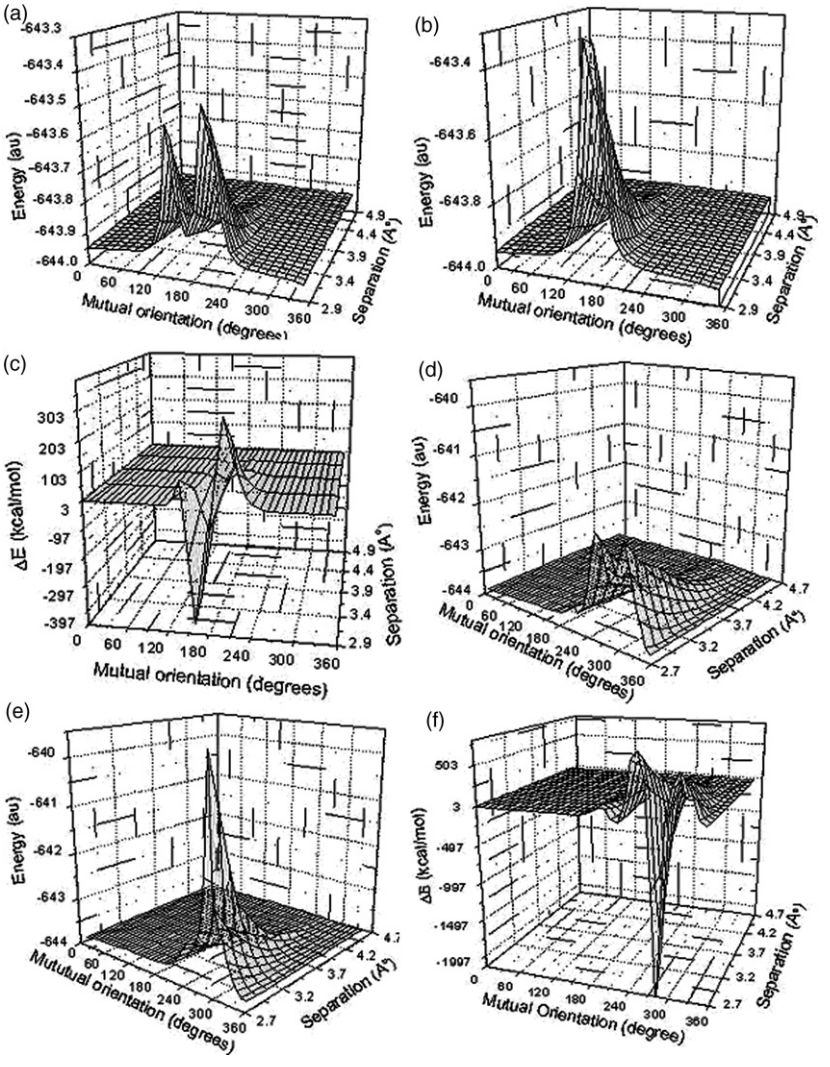

Figure 7. The *ab initio* (HF/6–311++G**) potential energy surface of (a) a pair of neutral L–L alanine molecules (b) a pair of neutral D–L alanine molecules as a function of orientation and distance (see reference [97] for details) (c) the chiral discrimination energy (ΔE_{LL-DL}) calculated from the potential energy surface of pairs of neutral L–L and D–L alanine molecules (d) a pair of zwitterionic L–L alanine molecules (e) a pair of zwitterionic D–L alanine molecules as a function of orientation and distance (f) the chiral discrimination energy (ΔE_{LL-DL}) calculated from the potential energy surface of pairs of zwitterionic L–L and D–L alanine molecules. All calculations are carried out with rigid geometry starting from optimised structure of the corresponding pair (reprinted from reference [97] with permission from the American Chemical Society. © American Chemical Society).

revealed that the intermolecular energy surface of the L–L pair is more favourable than the corresponding energy surface of the D–L pair. The study, for the first time, reveals homochiral preference without use of parameters, which was unobserved in previous detailed simulations but predicted by theory. The study suggests a possible method of

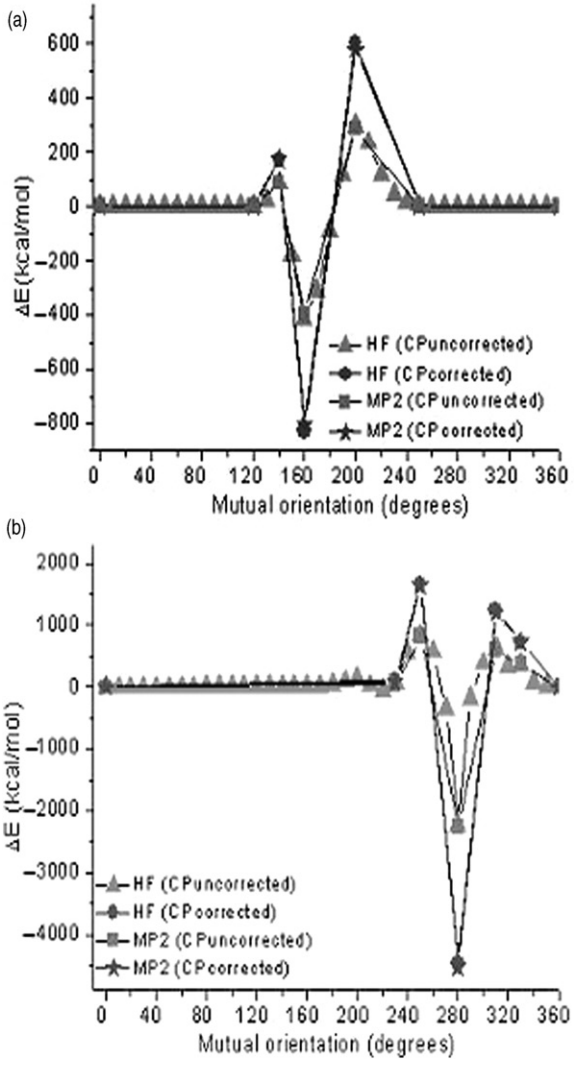

Figure 8. Comparison of the counterpoise-corrected result, which is BSSE free (denoted by $CP_{Corrected}$), and uncorrected result (denoted by $CP_{Uncorrected}$) of the slice of the chiral discrimination energy for (a) neutral and (b) zwitterionic alanine molecules. The plots correspond to the distance at which the maximal homochirality and heterochirality are observed in the respective uncorrected energy surfaces. Similarly, the line with filled squares indicates the energy plot for the BSSE uncorrected profile using chiral discrimination energy values at the MP2/6-311++G**. The line with asterisks indicates the energy plot for the BSSE corrected profile of chiral discrimination energy values at the MP2/6-311++G** (reprinted from reference [97] with permission from the American Chemical Society. © American Chemical Society).

D-amino acid exclusion. This is due to the larger degree of steric hindrance between D- and L-amino acid themselves rather than the L–L pair and concomitant homochiral preference. The electrostatic interaction of the homochiral pair further augments the homochirality in the case of the zwitterionic pair. The study indicates that chiral discrimination in peptide

synthesis can arise, at least partly, from the interaction between amino acids themselves as a function of intermolecular separation and orientation when the two amino acids are restricted to follow a rotatory path as occurring during peptide synthesis when A- and P-terminals are covalently linked to the tRNA structure and are not allowed to assume all possible mutual orientations. The result can be correlated with the observed discrimination noted in model systems like puromycin where the amino acids are not confined by surrounding residues.

The foregoing study is extended to consider the effect of surrounding of the PTC as well as the rotatory path followed by two terminals in a model of PTC from crystal structure of *H. marismortui* using hybrid quantum chemical studies [99]. The crystal structure of CCA-Phe-cap-biotin bound simultaneously at half occupancy to both the A-site and P-site of the 50S ribosomal subunit [100] is used to generate the molecular segments used in theoretical calculation [99]. Residues located in close proximity to the A- and P-terminals during rotation are as follows (all numberings correspond to scheme as in *Haloarcula marismortui*): phenyl alanine at A-terminal, phenyl alanine at P-terminal, A2485, A2486, C2487, A2488, U2620, A2637, G2540, U2451 and C2452. This is shown in Figure 4. In the calculations, phenyl alanine at A-terminal has either L-(natural) or D-configuration and phenyl alanine at P-terminal has L-configuration.

Experimental studies indicated that the 3′ ends of the A- and P-site tRNA have to face each other to result in the proper stereochemistry of the formed peptide bond. A process of spiral rotation of the 3′ end of the tRNA achieves this. The outcome of this spiral motion is that a P-site carbonyl carbon atom faces the A-site nucleophilic amine. This occurs without any significant conformational alterations of the 3′ end. In this calculation, starting from the mutual arrangement of A- and P-terminals in crystal structure, the A-terminal is oriented clockwise by an angle of 60° and anticlockwise by an angle of 60° in 10° increments covering a total range of orientation of 120° to simulate the rotatory motion of terminals in PTC.

The result exhibits a homochiral preference as the interaction of the L–L pair can happen at significantly lower energy and without any steric constraint over the range of orientation as shown in Figure 9. The D–L pair interaction is relatively unfavourable and corresponding energy profile has two minima only at limited range of orientations. The orientational space for D–L is limited which causes more steric clash with surrounding residues compared to the L–L pair. This is clear evidence of homochiral preference. This is the first quantitative calculation showing chiral discrimination in PTC. In order to understand the origin of the observed discrimination, different surrounding residues are removed and the influence on the ease of the rotatory path is studied. Exclusion of the U2620 from the surrounding residues drastically diminishes the discrimination. This is shown in Figure 10. This indicates that the U2620 has preferential non-bonded interaction with A- and P-terminal in L–L form rather than D–L form. However, homochiral preference is still significant as shown in Figure 10(b), where the scale is enlarged. Entire preferred homochirality, as observed in experiment and calculated as in Figure 9, is not due to U2620 and is non-negligible. All other residues are successively removed (A2485, A2486, C2487, A2488, A2637, G2540, U2451 and C2452) in order to identify the origin of residual discrimination and this is noted to change little from that observed in Figure 10(b). It may be noted that removal of backside residues such as A2485, A 2486, C2487 and A2488 gradually diminish the repulsive steric constraint in the range of 0° orientation but

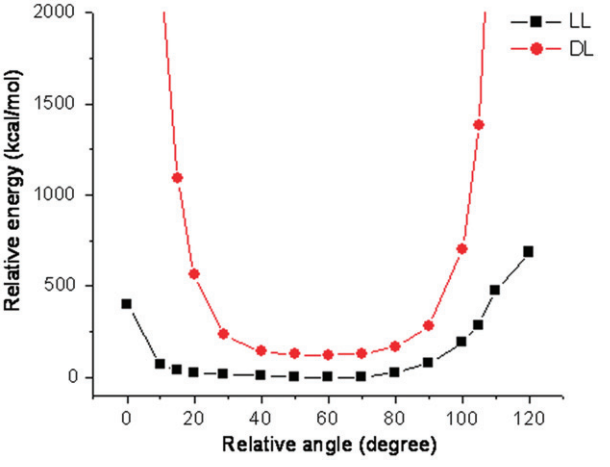

Figure 9. [Colour online] The variation in interaction energy as a function of orientation of phenyl alanine at A-terminal and phenyl alanine at P-terminal in presence of A2485, A2486, C2487, A2488, U2620, A2637, G2540, U2451 and C2452 residues as shown in Figure 2 for L–L and D–L pair combinations of two terminals. Starting from the mutual arrangement of A- and P-terminals in crystal structure, the A-terminal is oriented clockwise by 60° and anticlockwise by an angle 60° in 10° increments covering a total range of orientation of 120° (reprinted from reference [99] with permission from the American Chemical Society. © American Chemical Society).

discrimination remained effectively unchanged as observed in Figure 10. Finally, all residues are removed and two phenyl alanine groups are rotated without any surrounding residues in the same specified range of rotation. Interestingly, the discrimination is non-vanishing as shown in Figure 11. Strong homochiral preference is still noted in the range of mutual orientation (particularly at orientation close to 120°). The homochiral preference in the later range of orientation is entirely determined by the amino acid side chains. Comparison of the relative energy gap of L–L and D–L pair with all surrounding residues included except U2620 and the relative energy gap of L–L and D–L pair with all surrounding residues removed clearly shows that the residual discrimination (as remained after the removal of U2620) remained the same in the specified range of orientation and is independent of other residues. In fact, discrimination close to 120° is largely independent of any residues as shown in Figures 11 and 12 where the relative energy gap of L–L and D–L pair with all surrounding residues included and the relative energy gap of L–L and D–L pair with all surrounding residues removed are compared.

This conclusion corroborates the results of a previous study based on *ab initio* and DFT studies on the interaction of alanine molecules where homochiral preference is noted as a function of mutual orientation [97]. The study quantitatively shows that the observed homochiral preference is due to U2620 residue as well as the amino acid side chain at the A- and P-terminals. A major part of the discrimination comes from the variation of non-bonded interaction of rotating A-terminal with U2620 during approach of the former towards P-terminal. However, significant discrimination is due to the difference in the side chain interaction of A- and P-terminals themselves during the rotatory motion.

It is important to address how important is the chirality of the D-sugar in the context of the long-length scale structural organisation of the PTC. Explicitly, whether the possible

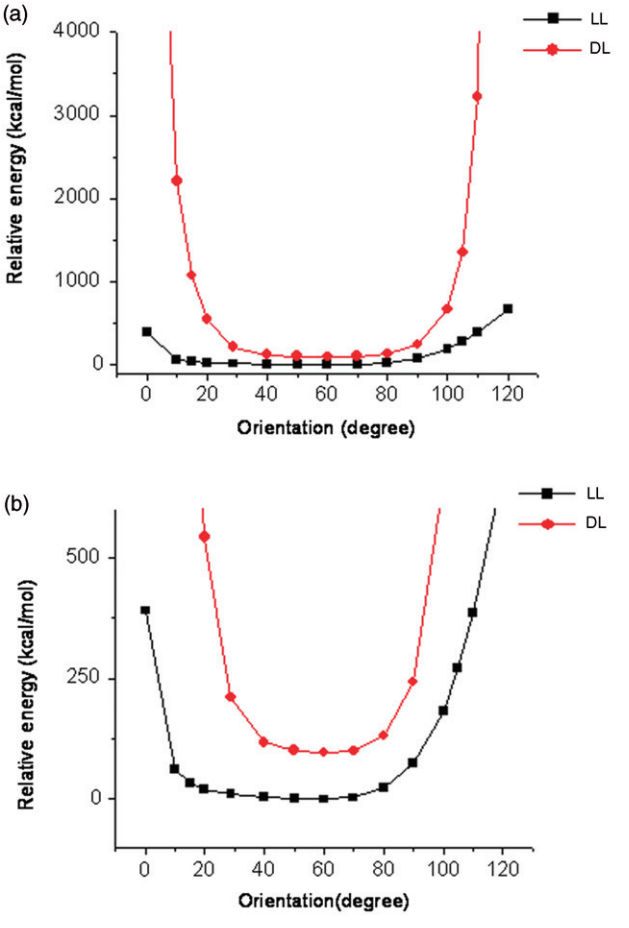

Figure 10. [Colour online] (a) The variation in interaction energy as a function of orientation of phenyl alanine at A-terminal and phenyl alanine at P-terminal in presence of A2485, A2486, C2487, A2488, A2637, G2540, U2451 and C2452 residues and excluding U2620 for L–L and D–L pair combinations of two terminals. Starting from the mutual arrangement of A- and P-terminals in crystal structure, the A-terminal is oriented clockwise by 60° and anticlockwise by an angle 60° in 10° increments covering a total range of orientation of 120° (b) the discrimination remained after removal of U2620 is highlighted (reprinted from reference [99] with permission from the American Chemical Society. © American Chemical Society).

heteropairs and homopairs (other than the D-sugar and L-amino acid) can perform the peptide synthesis with similar efficiency in natural biological surroundings (PTC). As the enantiomers differ only in the mutual spatial arrangement of groups, the changes in the spatial interactions in other heteropair and homopair combinations within the PTC may be negligible for discrimination. Whether such changes in spatial orientation have any influence on effective peptide synthesis needs to be addressed. Several complementarities of the sugar chirality with amino acid and the surrounding bases can exist, which might have favourable contribution of the D-sugar ring to the process of chiral discrimination in

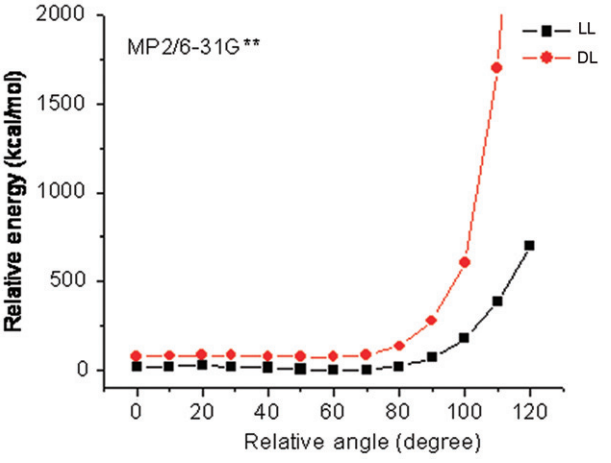

Figure 11. [Colour online] The variation in interaction energy as a function of orientation of phenyl alanine at A-terminal and phenyl alanine at P-terminal for L–L and D–L pair combinations of two terminals without any surrounding residue. Starting from the mutual arrangement of A- and P-terminals in crystal structure, the A-terminal is oriented clockwise by an angle of 60° and anticlockwise by an angle of 60° in 10° increments covering a total range of orientation of 120° (reprinted from reference [99] with permission from the American Chemical Society. © American Chemical Society).

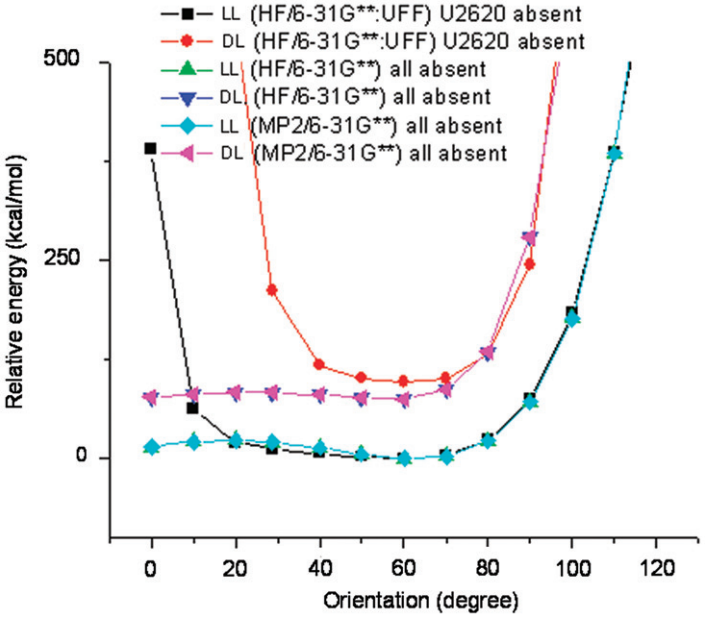

Figure 12. [Colour online] Comparison of the relative energy gap of L–L and D–L pair with all surrounding residues inclusive except U2620 (as shown in Figure 3) and the relative energy gap of L–L and D–L pair with all surrounding residues removed (as shown in Figure 4). It is important to note that the absolute energy values as shown in Figure 3 and those in Figure 4 are different and the lowest energy level of two plots are brought to the same level in Figure 5 to note the relative energy gap of L–L and D–L pair (reprinted from reference [99] with permission from the American Chemical Society. © American Chemical Society).

peptide synthesis. As mentioned in Section 1, the molecular understanding of the origin of the chiral specificity of the sugar ring (D-form rather than L-form) in nucleic acid structure and its role in controlling the fidelity of the peptide synthesis is important. Experimental studies of Hecht [90] indicated that while *N*-acetyl-D-phenylalanyl-tRNA^{Phe} and *N*-acetyl-D-tyrosyl-tRNA^{Phe} produced only small amount of dipeptide, the 2′ and 3′ deoxyadenosine analogues produced no detectable dipeptide formation. This indicates that the discrimination in peptide synthesis is coupled with the D-form of sugar. These possibilities have been explored recently [101]. First, it might have favourable stereochemistry related to the structural organisation of tRNA. Second, the sugar ring might have the proper stereochemistry that can make the rotatory path (in which the A-site tRNA 3′-end flips into the P-site by rotating around the bond connecting the single strand 3′-end) leading to easier optimal orientation for peptide bond formation. Third, the hydroxyl group attached to 2′ can catalytically lower the transition state barrier (related to the formation of the peptide bond) when positioned in a favourable stereochemical orientation.

Recent modelling shows that changes in the chirality of the sugar ring brings large-scale structural changes in tRNA structure, which is unfavourable for the peptide synthesis process [101]. Model building indicates that the unnatural combinations of amino acid and sugar (L-amino acid: L-sugar, D-amino acid: D-sugar and D-amino acid: L-sugar) within the model of PTC from the crystal structure of the 50S ribosomal subunit of the *H. marismortui* (PDB ID: 1Q86) are unfavourable to make proper stereochemistry to form a peptide bond within the PTC as well as creating steric hindrance. Large-scale structural rearrangement is required to accommodate these unnatural pairs [101]. Exchanging the C5′ with any other atom or group leads to a change in the orientation of the phosphodiester backbone. This is energetically unfavourable. Similarly, change in the chirality at C1′ will lead to a change in the orientation of bases and will affect the base pairing. The result indicates that the naturally available PTC is highly chirality specific and can accommodate only the natural heterochiral pair of sugar and amino acid without any large-scale structural change in tRNA.

The variations of energy as a function of orientation in the rotatory path by which the two terminals approach each other are also studied in presence and absence of the sugar ring and are compared [101]. The computation explores the relative ease of the variation of energy as a function of orientation in the rotatory path in the presence and absence of the sugar ring. The ONIOM calculation is performed at (HF/6-31G**: UFF). The variation in energy in going from the lowest energy point in each model (with sugar ring and without sugar ring) is considered as a function of orientation and taking the lowest energy of each model as zero is as shown in Figure 13. The plot shows that the presence of a sugar ring in both terminals makes the rotatory path more favourable compared to the case when the sugar ring is removed. Since rotation of the A-terminal occurs around the 3′ bond, the rotatory process is an orientational motion of the amino terminal with respect to the A-site sugar ring. As a result, removal of A-site sugar ring raises the energy due to the loss of interaction. The contribution of the P-site sugar ring in stabilising the process is more than the A-site sugar ring. This result is consistent with the fact that as the A-site approaches the P-site, the interaction of the amino group of the A-site interacts with the peptidyl terminal and the sugar ring of P-site. This contributes to the orientation-dependent interaction. The interaction is lost with the removal of the ring and energy rises further. The result shows that the A- and P-site sugar rings have significant favourable influence in

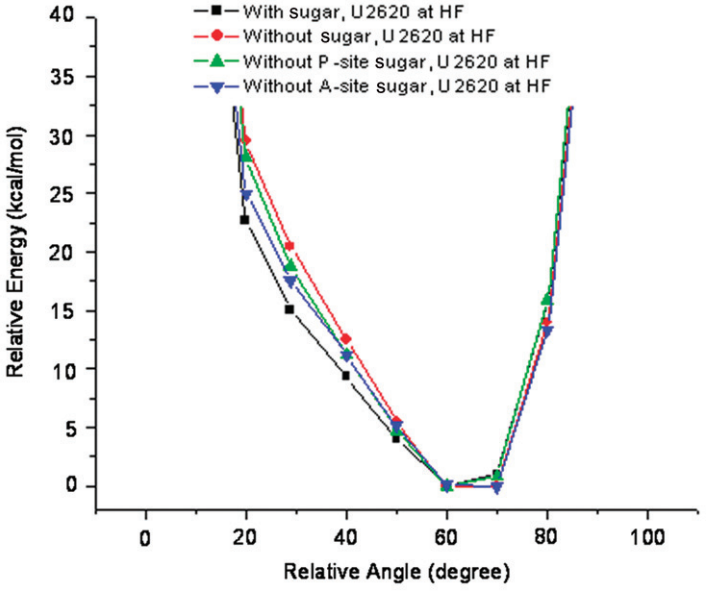

Figure 13. [Colour online] (a) The variation in interaction energy as a function of orientation of phenyl alanine at A-terminal and phenyl alanine at P-terminal in the presence and in absence of sugars attached to A-76 attached to both terminals and within a model of PTC. Starting from the mutual arrangement of A- and P-terminals in crystal structure, the A-terminal is oriented clockwise by an angle of 60° and anticlockwise by an angle of 60° in 10° increments covering a total range of orientation of 120°. The ONIOM calculation is performed at (HF/6-31G**: UFF). The phenyl alanine at A-terminal, P-terminal and U2620 is considered at QM level. The residues other than U2620 included in model are considered at UFF level (b) the variation in interaction energy as a function of orientation of phenyl alanine at A-terminal and phenyl alanine at P-terminal in the presence and in absence of sugars of only A-site and P-site, respectively (reprinted from reference [101] with permission from the American Chemical Society. © American Chemical Society).

the rotatory path. It further indicates that the combined presence of D-sugar and L-amino acid makes the rotatory path more favourable compared to the structure in which the D-sugar is absent.

The role of the microscopic chirality of the sugar ring and specifically that of the 2′ chiral carbon of the A76 (where the OH group, suggested to have a catalytic role, is attached) seems important. Its catalytic role in the peptide synthesis is explored recently [101]. Experimental studies indicate that the hydroxyl group is responsible for the significant high rate of the peptide synthesis in ribosome compared to that of an uncatalysed one (in absence of ribosome). The catalytic mechanism of the involvement of the 2′ OH group of the sugar ring remains a question. The role of 2′ OH in the peptide synthesis was suggested a while ago [102]. A comparison of the activities of 2′ deoxy derivative of AcLeuAMP, AcLeuAMP derivative with either a second AcLeu at the 2′ OH or with a 2′ OCH_3 at the 2′ position of ribose indicates that the activity of the deoxy substrate is at least 100-fold lower than the substrates containing active 2′ hydroxyl group [103]. Substitution of the P-site *t*-RNA A76 2′ OH with 2′ H or 2′ F resulted in 10^6-fold decrease in the peptide bond formation [104]. It is noted that the rate effect is inconsistent

with the pH-dependent catalytic mechanism and the role of the 2′ OH could be orienting the nucleophile, stabilisation of the transition state or inducing a favourable catalytic conformation of the PTC [105]. It is proposed that it facilitates the peptide bond formation by substrate positioning and acts as a proton shuttle between the amino group of A-site t-RNA and the A76 3′ oxygen atom of the ester bond of the peptidyl t-RNA. A study of modified substrates and mimics of intermediates indicates that 2′ OH can serve as a proton shuttle [106]. A proton shuttle is proposed in which the 2′ OH receives a proton from the attacking amino group and simultaneously donates the proton to the neighbouring 3′ OH as the transition state is decomposed into product [107]. It is proposed that the catalytic effect is due to the stable hydrogen bond network observed along the reaction. However, other catalytic pathways involving 2′ OH are possible. First, it is possible that the amino group attacks the ester carbon to yield the tetrahedral intermediate, which breaks down to deacylated tRNA and elongated peptidyl tRNA. Second, it is possible that the zwitterionic intermediate may break down through a proton shuttle via the 2′ OH of A76 in the P-site in stepwise or concerted pathway and finally, the proton shuttle may involve a water molecule that interacts with 2′ and 3′ hydroxyl of A76 [108]. Recent detailed quantum mechanical calculation of the transition state also emphasised the role of increase in the hydrogen bonding between the transition state geometry and the ribosomal components in stabilising the transition state [109]. It is suggested that the 2′ OH group of the sugar ring remains in close interaction with the A-site amine and carbonyl group during the rotatory path leading to peptide bond formation through substrate-assisted catalysis, which is different from the proton shuttle mechanism discussed earlier. The role of the 2′ OH group into the rate enhancement produced by the ribosome based on entropic contribution is proposed [110,111]. These studies indicate that the stereochemistry of the 2′ chiral carbon facilitates the reaction by catalytic mechanism using the OH group despite the fact that the two mechanisms are found to be competitive.

The relative barrier height of the transition state for the formation of a peptide bond and the influence of the 2′ OH group has been recently studied for two different mechanisms (proton shuttle and anchoring mechanism) [101]. Comparison of the transition state barrier height in the presence and absence of the 2′ OH group is shown in Figure 14. The difference can be attributed to the removal of the chirality of the 2′ carbon of the sugar ring. The transition state geometries with and without 2′ OH are shown in Figure 15(a) and (b), respectively. The difference in barrier heights in the two cases is 21.27 k cal/mol at the HF/3-21G level of theory. This qualitatively indicates that the change in the stereochemistry of the 2′ centre can alter the progress of the synthesis by several orders of magnitude. The observation corroborates the experimental data that the substitution of P-site tRNA 2′ OH by 2′ H and 2′ F results in a 10^6-fold reduction in the rate of peptide bond formation [104]. A comparison of the transition states in the two cases indicates that the anchoring role of the 2′ OH group is responsible for lowering the barrier height compared to the case when the 2′ OH group is removed. The result strongly suggests that the chirality of the 2′ carbon is vital for the rate enhancement.

If the proper orientation of the 2′ OH and anchoring by it is responsible for the effective catalytic role in the reaction, then change in the orientation of the group will lead to a diminishing rate. Alteration of the stereochemistry at the 2′ centre of sugar ring results in rise of the barrier height. The result indicates that the change in the stereochemistry of the 2′ OH makes the process as unfavourable. The rate diminished less than the case when

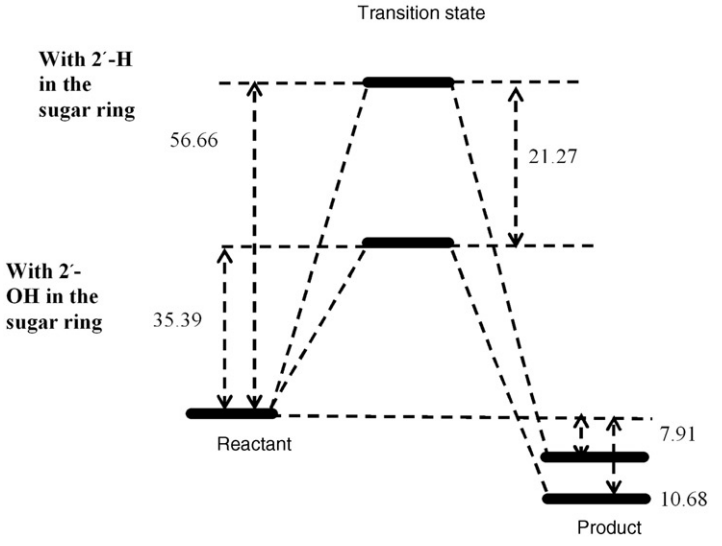

Figure 14. Comparison of the transition state energy level diagrams of L–L phenylalanine peptide bond formation reaction with and without the 2′ OH of the sugar rings at HF/3-21G level of theory. The relative energies (with respect to the respective reactants and later values taken as zero) are expressed in kcal/mol (reprinted from reference [101] with permission from the American Chemical Society. © American Chemical Society).

the OH group is completely removed. This indicates that the proper positioning of the group and natural chirality is vital for the reaction. The stereochemical orientation of the hydroxyl group is changed when the chirality at 2′ carbon is either altered or removed. This affects the proximal geometry for the catalytic process and leads to the reduction in the rate of peptide synthesis, which is consistent with the experimental studies [104].

The geometries of the calculated transition states as obtained from models built from ribosomal parts of *H. marismortui* using HF calculations [101] and the transition state structure obtained from density functional calculations based on a model from crystal structure of 50S large ribosomal subunit from *Deinococcus radiodurans* complexed with a tRNA acceptor stem mimic (PDB ID: 1NJP) [109] compare reasonably. The result of the calculation based on crystal structure from *H. marismortui* and those obtained based on crystal structure from *D. radiodurans* using density functional theories compare fairly well [101] considering the different systems and theoretical methods employed. However, other mechanisms for catalytic activity are also proposed. A concerted proton shuttle from A-site N to 2′ O to 3′ O of P-site is suggested by other workers [107,112,113]. The barrier height related to the transition state involving a proton shuttle and anchoring mechanisms are comparable [101].

Origin of the influence of sugar chirality on the rate of the reaction can be understood from the transition state geometry. It is noted that during the nucleophilic attack at the P-site, one of the hydrogen atoms attached to the α-amino group of the amino acyl-tRNA at the A-site is in proximity of carbonyl carbon (–NH $\cdots$ O=C– distance is 2.09 Å) and the other one is also close to the oxygen atom of the 2′ OH of the P-site sugar ring (–NH $\cdots$ O–C– distance is 2.39 Å). The hydrogen atom of the 2′ OH of the P-site sugar ring is at a

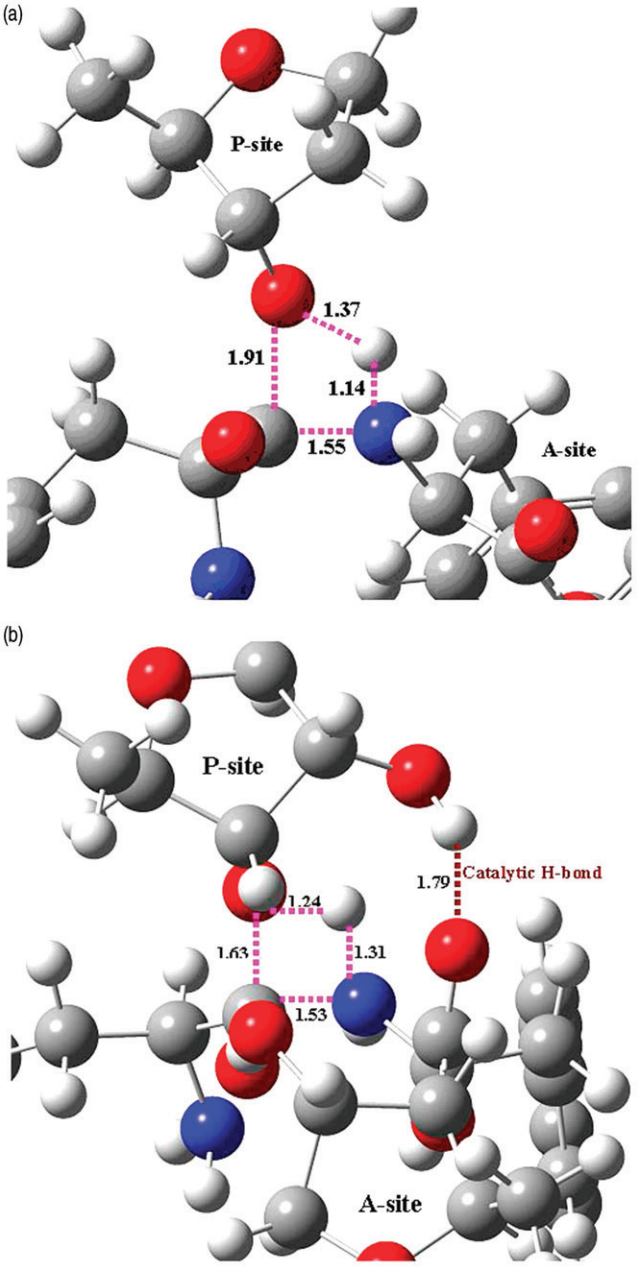

Figure 15. [Colour online] Comparison of the transition state geometries of L–L phenylalanine peptide bond formation reaction (a) without 2′ OH of the sugar rings at HF/3-21G level of theory (b) with the 2′ OH of the sugar rings at HF/3-21G level of theory (reprinted from reference [101] with permission from the American Chemical Society. © American Chemical Society).

distance of 3.34 Å from the oxygen atom of the ester bond of the peptidyl-tRNA at the P-site. Thus, the reactant geometry contains a cycle of hydrogen bonds and the hydrogen bond distances are further shortened in the transition state geometry. Several of these hydrogen bonds are absent when the 2′ OH is removed. The corresponding transition state (in the absence of 2′ OH) contains a hydrogen bond of distance 1.37 Å between the A-site α-amine hydrogen and P-site 3′ oxygen atom of the ester bond. The result indicates that all catalysing bonds present in the transition state structure containing the P-site 2′ OH are absent in the corresponding structure when 2′ centre is achiral. While the proton shuttle and anchoring mechanisms differ substantially, both lower the transition state energy compared to the case when the chirality of the 2′ carbon is either altered or removed. This can be followed from the geometries of the corresponding transition states (where the OH group is taking part in a proton shuttle and where the OH group acts as anchor). The corresponding geometries are shown in Figures 16(a) and (b), respectively.

The surrounding residues present in the PTC (which are in nanometer length scale proximity with the D-sugar) also influence the rotatory path and the discrimination. Although the bases are achiral, their interaction with the sugar ring can be orientation dependent and can influence chiral discrimination. It was pointed out earlier that, when achiral moieties have restricted orientational freedom, its interaction profile with a chiral moiety can be orientation dependent [34]. This orientation dependence can be different for the L- and D-form of the chiral moiety and might give rise to discrimination. The influence of various surrounding residues such as C2104, C2105, A2485, A2486, C2487, U2541, C2542, C2608, G2618, U2619, U2620 and A2637 on the rotatory path and their interaction with the sugar ring related to the A-site and P-site of the 50S ribosomal subunit of *H. marismortui* has been investigated recently [101]. The removal of the surrounding residues affects the non-bonded interaction with the amino acid: sugar heteropair of natural chirality. Previously it was noted that the U2620 at PTC has important influence on the discrimination between the L–L pair and D–L pair arising from the consideration of the rotatory path related to the approach of two terminals leading to peptide bond formation. The removal of the U2620 diminished the discrimination indicating that U2620 has favourable interaction with the L-terminal rather than D-form of the terminal. The removal of U2620 affects the rotatory path to form a peptide bond as shown in Figure 17. The removal makes the loss of interaction between sugar ring and U2620 for a certain range of orientation and hence the energy rises in the absence of U2620. The effect of removal of A2486 on the rotatory path is presented in Figure 18(a). The result shows loss of favourable intermolecular interaction in the range of orientation in which the rotating A-site is in proximity of the base when the latter is removed. Similar loss of intermolecular interaction is noted by removing the G2618 as shown in Figure 18(b). On the other hand, removal of C2487, U2541, C2104, C2105, A2485, C2542, C2608, U2619, A2637 and U2541 shows no significant loss of intermolecular interaction. These results indicate that, while a set of surrounding residues have favourable influence on the peptide bond formation between A- and P-terminals within PTC, a number of other residues might have less influence on the same process. However, more detailed study using higher level theory and basis set is necessary.

The foregoing computational studies reveal that the molecular mechanism of the chiral discrimination involves the A- and P-amino acids, D-sugar ring and surrounding bases of the PTC. Several factors are noted to be responsible for the discrimination and explain the

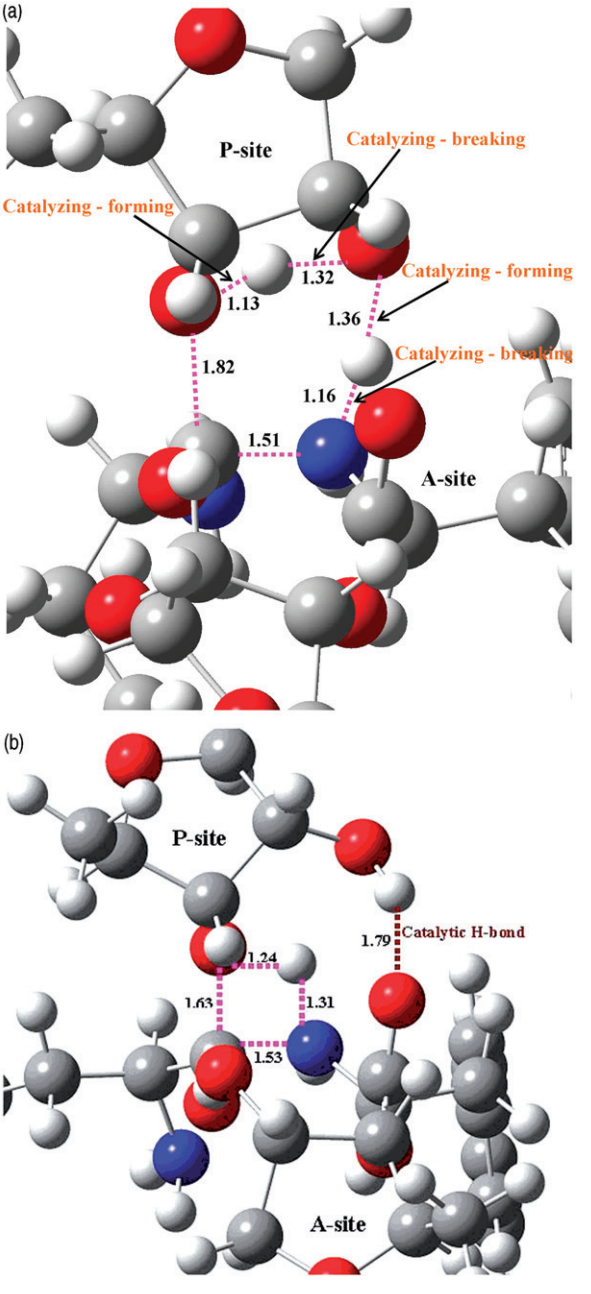

Figure 16. [Colour online] Comparison of the transition state geometries of L–L phenylalanine peptide bond formation reaction with 2′ OH of the sugar ring with (a) proton shuttle and (b) anchoring mechanism at HF/3-21G level of theory (reprinted from reference [101] with permission from the American Chemical Society. © American Chemical Society).

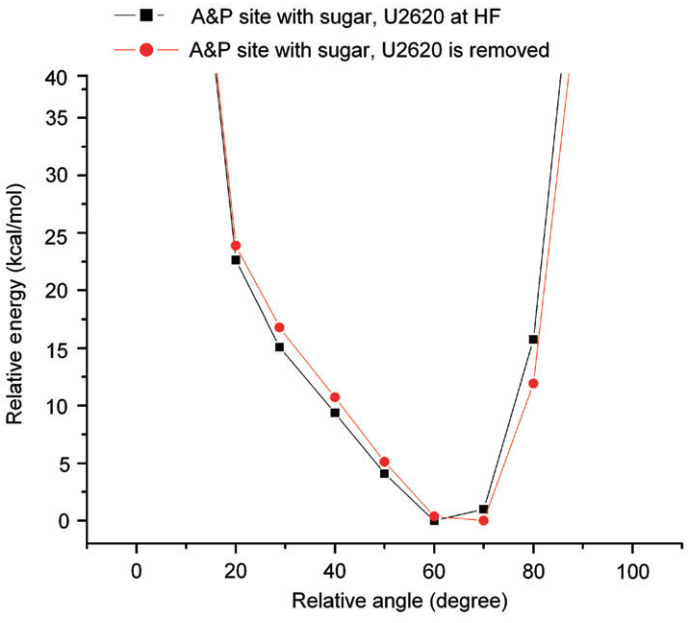

Figure 17. [Colour online] Variation in interaction energy as a function of orientation of phenyl alanine at A-terminal and phenyl alanine at P-terminal in the presence and in absence of U2620, respectively (reprinted from reference [101] with permission from the American Chemical Society. © American Chemical Society).

high level of stereospecificity of the process. The factors can be listed as follows: (1) the chiralities of the amino acids at A- and P-terminals are most important. The rotatory path for the approach of D-amino acid towards the L-terminal is unfavourable due to steric hindrance between the amino acids themselves. Their nanoscale separation is important for discrimination and, at larger separation, no discrimination is noted. (2) The restricted nature of the mutual orientation between the terminals during the rotatory path for the approach to form the peptide bond makes the resultant interaction profile different for the L–L and D–L pair exhibiting discrimination. (3) The natural chirality (D-form) of the sugar ring has favourable influence on the long-length scale organisation of tRNA. Alteration of the chirality of the sugar ring is unfavourable as it requires large structural rearrangements of tRNA. (4) Favourable influence of the D-sugar ring on the rotatory path for approach to form the peptide bond is noted. The removal of the sugar ring makes the rotatory path for approach to form the peptide bond unfavourable, which indicates that the interaction of the D-sugar with the amino acids is more favourable than other homo- or heteropair combinations of sugar–amino acid. (5) The stereochemistry of the 2′ centre of the D-sugar is vital as it catalyses the peptide bond formation by making proper placement of the OH group, which is involved in the catalysis. The analysis of the transition state structure revealed that the alteration and removal of chirality of the 2′ centre destabilise the transition state and makes the formation of a peptide bond unfavourable. (6) The nanoscale proximity of some of the surrounding bases present in PTC with the A- and P-terminals and their restricted orientation have influence on the discrimination.

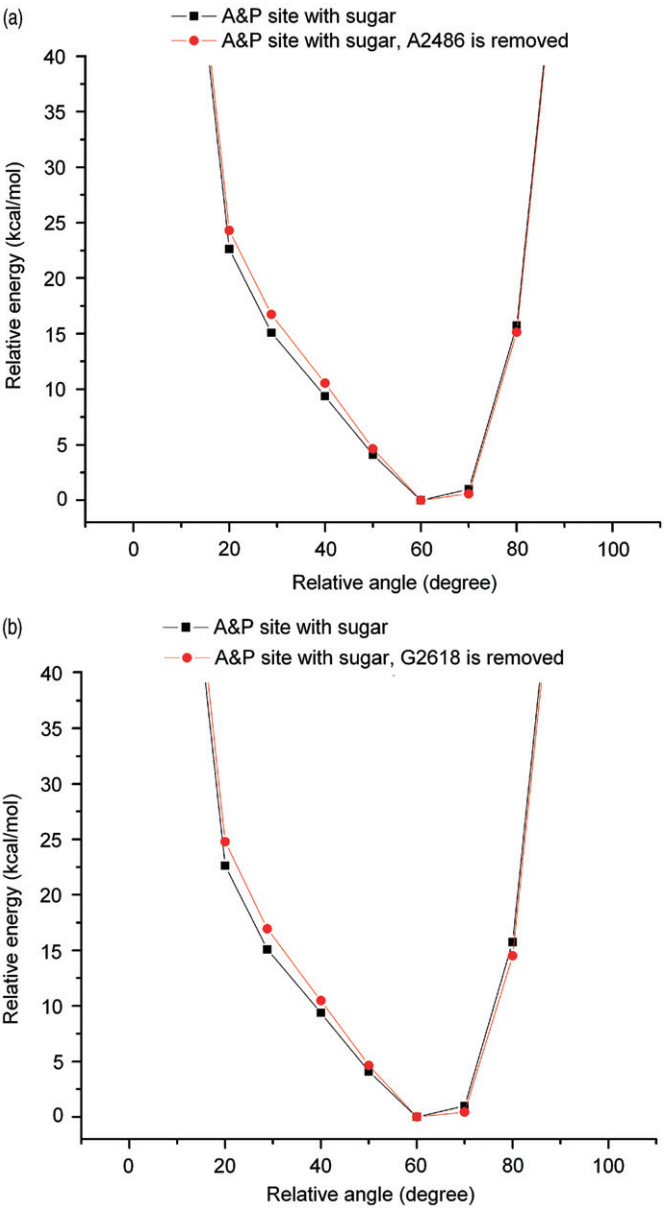

Figure 18. [Colour online] (a) Variation in interaction energy as a function of orientation of phenyl alanine at A-terminal and phenyl alanine at P-terminal in the presence and in absence of A2486, respectively. (b) Variation in interaction energy as a function of orientation of phenyl alanine at A-terminal and phenyl alanine at P-terminal in the presence and in absence of G2618, respectively (reprinted from reference [101] with permission from the American Chemical Society. © American Chemical Society).

Thus, multiple factors control the discrimination in the peptide synthesis and allowed accurate retention of the biological homochirality.

Other vital steps of the protein synthetic pathway, like aminoacylation reaction, precede the peptide bond formation, which also exhibits chiral discrimination. Aminoacylation is a key step in the natural biosynthesis process of peptide, which connects the realm of protein with the RNA world. Incorrect aminoacylation might lead to misacylation of D-amino acid in the tRNA, which might cause synthesis of a hetero-peptide rather than natural homopeptide. In the following, we discuss the experimental and computational studies, which show that chiral discrimination in aminoacylation is stringent.

4. Chiral discrimination in the aminoacylation reaction in the aminoacyl transferase: experimental studies

As noted in Sections 2 and 3, respectively, successful and strong chiral discrimination in peptide synthesis depends on the chirality of amino acids, sugars, proximity between them and interaction with the residues present in the confined environment of the surrounding nanospace of PTC. The aminoacylation reaction also involves chiral amino acids and sugars, and occurs within the active site of aminoacyl transferase, which is composed of chiral amino acids rather than the achiral surrounding environment as present in PTC. These residues are located within a nanoscale distance. Hence, the aminoacylation reaction involves a number of factors that lead to the manifestation of chiral discrimination. Indeed, the specificity of the AARSs to incorporate a specific amino acid and its ability to discriminate between several competing substrates is well known [114]. The ability to discriminate among amino acids, which may differ only in a subtle way, is one of the major requirements for accurate translation of the genetic code. The frequency of disincorporation of non-cognate amino acid is 1 in 10^4, which is a surprisingly accurate [115]. A Michaelis–Menten enzyme substrate interaction is not adequate to explain such specificity. There may be a succession of discriminating processes [116,117]. Synthetase ensures that only cognate substrates are selected from the large cellular pool of similar amino acids or tRNA.

It is suggested that a number of intricate contacts between AARS and amino acid, which is favourable for cognate but unfavourable for non-cognate amino acids, makes the successful recognition and concomitant discrimination [114]. Most of the aminoacyl-tRNA contains an editing site in addition to an acylation site. These complementary pairs of sites function as a double filter to ensure that non-cognate amino acids are rejected. It is proposed in literature that the acylation site rejects amino acids larger than the correct one because there is insufficient space for them. On the other hand, the smaller amino acids are cleaved by the hydrolytic editing site [115]. However, this size- or volume-based mechanism is not capable of discriminating the enantiomeric species of the cognate amino acid as the D- and L-enantiomers occupy identical total volume. The fact that the discrimination of cognate and non-cognate amino acids is achieved by a number of interactions between AARS and amino acid is responsible for the recognition of cognate amino acids that is explored by several workers. Each synthetase has a specific molecular mechanism to distinguish the correct pair of substrates from the pool of amino acids and tRNA molecules.

The mechanism of the selection of amino acids is studied by a number of workers by various methods. However, the studies on chiral discrimination are limited. Archontis *et al.* [118] studied how aspartyl-tRNA synthetase distinguishes between negatively charged aspartic acid and neutral asparagines using molecular dynamics simulation and free energy simulation. To correctly account for the electrostatic interactions in the system (including bulk solvent), the region of the mutation site is treated microscopically, whereas distant protein and solvent are treated by continuum electrostatics. The substrate Asp is predicted to bind much more strongly than Asn, with a binding free energy difference of 15.3 kcal/mol. This implies that erroneous binding of Asn by AspRS is highly improbable. Almost all of the protein contributions to the Asp *versus* Asn binding free energy difference arise from an arginine and a lysine residue that hydrogen bonded to the substrate carboxylate group and an Asp and a Glu. These four amino acid residues are completely conserved in AspRSs. The protein effectively 'solvates' the Asp side-chain more strongly than water does. Some synthetases discriminate between amino acids by forming a network of interactions between the amino acid and its specificity pocket, as has been explicitly shown in CysRS and TyrRS [119–121]. The mechanism by which glutaminyl-tRNA synthetase (GlnRS) recognises $tRNA^{Gln}$ and ATP is also well established [122–124]. In the case of glutaminyl-tRNA synthetase (GlnRS) to discriminate glutamic acid or glutamate, both hydrogen atoms of the nitrogen of the glutamine side chain are recognised [125]. The hydroxyl group of a tyrosine (tyr211) and a water molecule are responsible for this recognition; both serve as hydrogen-bond acceptors due to the presence of a network of interacting side chains and water molecules. These results indicate that the hydrogen bonded interaction of the amino acid residues in the active site with the amino acid substrates is important for discrimination.

Ionic interactions are also responsible for the selection of amino acid. Cysteinyl-tRNA synthetase (CysRS) is highly specific for synthesis of cysteinyl adenylate, yet does not possess the amino acid editing activity, which is characteristic of many other tRNA synthetases. Crystal structures of the *E. coli* enzyme reveal that the substrate cysteine thiolate forms a single direct interaction with a zinc ion bound at the base of the active-site cleft, in trigonal bipyramidal geometry together with four highly conserved protein side chains [126]. Cysteine binding induces movement of the zinc ion towards substrate, as well as flipping of the conserved Trp205 indole ring to pack on the thiol side chain. The imidazole groups of five conserved histidines lie adjacent to the zinc ion, forming a unique arrangement suggestive of functional significance. Amino acid discrimination without editing arises most directly from the favourable zinc-thiolate interaction, which is not possible for non-cognate substrates. Additional selectivity may be generated during the induced-fit conformational changes that help assemble the active site. This indicates that the confinement and proximity of residues are important in the recognition in the aminoacylation synthetase.

Experimental studies indicate that the specificity is present at the level sufficient to discriminate the enantiomeric species. Early studies indicated that when D-isomer is tested as substrates with particle-free supernatant of pancreas homogenate containing synthetase, no activity was observed [127]. Calender and Berg [128] investigated the substrate specificity of tyrosyl RNA synthetases of *E. coli* and *B. subtilis* and noted that D-tyrosine was activated and transferred to tRNA. A striking feature of a subsequent study is that L- and D-tyrosyl RNA can be formed at the same extent from L-or D-tyrosine, excess

tyrosyl RNA synthetase and limiting tRNA [83]. Partially purified preparations of alanyl-, leucyl- and valyl-RNA synthetases from *E. coli* and found that D-enantiomers were esterified to tRNA at $<10^{-5}$ the rate of L-enantiomers. Barely detectable amount of D-phenyl alanyl RNA is noted to be formed using phenylalanyl RNA synthetases and this was only 6×10^{-5} the rate found for L-phenylalanyl RNA. Tyrosyl RNA synthetases from *E. coli* and *B. subtilis* are unique in that they are the first enzyme that synthesise D-aminoacyl RNA derivatives.

Soutourina *et al.* [129] concluded that, in addition to D-tyrosine, D-enantiomers of other amino acids can be incorporated based on an investigation of *E. coli* and *Saccharomyces cerevisiae* systems. It is also pointed out that the deacylase activity might have a broader implication in retaining enantiopurity. The broad specificity of *E. coli* D-tyr-tRNA deacylase was early observed *in vitro* by Calendar and Berg [83]. The deacylase recognises very different D-aminoacyl moieties like the acidic aspartate or the bulky aromatic tryptophan. The authors discuss another important pathway of removal of the toxic D-amino acid in addition to the proof-reading mechanism during aminoacylation step. In the case of auxotrophic bacteria, the lack of many biosynthetic pathways might result in low levels of endogenous D-amino acids. The deacylase activity would be redundant in such bacteria. However, D-aminoacyl-tRNA deacylase activity would be necessary in other cells to reduce the harmful effect of D-amino acid transfer to tRNA. Deacylase should be present to hydrolyse any D-aminoacyl-tRNA molecule. Soutourina *et al.* have raised the question of why cells have maintained genes, which encode a deacylase capable of hydrolysing D-AA-tRNATyr into free tRNA-AA and D-AA (AA being amino acid like Tyr or other) rather than evolving through the selection of more specific aminoacyl-tRNA synthetases. It is suggested that the primitive cell might have indifferently incorporated L- and D-amino acids into polypeptides. At this stage, acquisition of a general D-aminoacyl-tRNA deacylase activity could have helped the cell to shift protein synthesis in the L-amino acid world. According to this situation, further evolution of cells implies an improvement of the specificity of the synthetases towards L-amino acids, and the progressive loss of a no longer useful deacylase gene, which becomes unnecessary. Cyanobacteria and archaebacteria may correspond to such cells. However, this proposition is yet to be verified.

Bergmann *et al.* [130] tested the specificity of L- and D-isomers of valine, isoleucine and leucine for aminoacyl adenylate formation with valyl, isoleucyl, leucyl and methionyl RNA synthetases. In all cases, the formation of the D-aminoacyl adenylate formation is negligible or nil compared to the corresponding L-aminoacyl adenylate formation. Similar chiral specificity is noted for aspartyl tRNA synthetase of *Lactobacillus aerabinosus* [131]. Yamane and Hopfield [117] observed that both L- and D-tyrosine can be esterified by tyrosine-tRNA synthetase. This conclusion corroborates the study by Calendar and Berg. The amount of ATP hydrolysed per tRNA acylated is practically identical for both enantiomers. Tyrosyl RNA synthetase is known to be non-specific with respect to the acylating position (2′ or 3′ position of hydroxyl group of adenosine moiety) and it is suggested that it may lack the 2′ hydrolytic activity of other synthetases. This may also explain the existence of D-Tyr tRNA deacylase and absence of enzymatic deacylation of D-Tyr-tRNA [117]. In a series of detailed studies, Hecht [90] demonstrated ways of preparation of tRNA activated with a variety of amino acids and amino acid analogues and the mechanism of aminoacylation is a different one from the natural process.

The discrimination noted in the peptide synthesis using such misacylation (including D-amino acid) is described in the previous section.

Profy and Usher [132] studied the aminoacylation of diinosine monophosphate (Inosinylyl-(3′–5′)-inosine) which is a model system with both 2′ and 3′ hydroxyl groups. When the acylating agent was the imidazolide of *N*-(tert-butoxycarbonyl)-DL-alanine, a 40% enantiomeric excess of the L isomer was incorporated at the internal 2′ site. The positions of equilibrium for the 2′–3′ migration reaction differed for the D and L enantiomers. In contrast, reaction of IpI with the imidazolide of unprotected DL-alanine led to an excess of the D isomer at the internal 2′ site, while reaction with the *N*-carboxy anhydride of DL-alanine proceeded without detectable stereoselection.

Tamura and Schimmel [133] studied the plausibility of chiral selectivity during the second step of aminoacylation by carrying out non-protein, non-ribozyme, RNA-directed aminoacylation of an RNA minihelix that recapitulates the domain within tRNA that harbours the amino acid attachment site. The minihelix^{Ala} is constructed as based on the sequence of *E. coli* tRNA^{Ala}, considered as a progenitor of modern tRNA. While natural systems use aminoacyl phosphate (mononucleotide) adenylates as intermediates for aminoacyl tRNA synthesis, the authors designed an aminoacyl phosphate oligonucleotide to hybridise to the 3′-end of the minihelix through a bridging oligonucleotide, thereby bringing together the activated amino acid and the amino acid attachment site. Minihelix^{Ala}, a bridging oligonucleotide, and 5′-[^{14}C]-L-Ala-p-dT_6dA_2 as well as 5′-[^{14}C]-D-Ala-p-dT_6dA_2 are mixed together to achieve aminoacylation of minihelix^{Ala}. The 3′ terminal A was replaced by either 2′-dA or 3′-dA. While the 2′-dA substrate was charged, the 3′-dA derivative was not. Thus, aminoacylation was specific for the 3′-OH. Formation of the [^{14}C]L-Ala-minihelix is preferred over that of [^{14}C]D-Ala-minihelix by a ratio of about 4:1. Both stereoisomers of Leu-p-dT_6dA_2 and of Phe-p-dT_6dA_2 are also tested for chiral selectivity. A clear preference for L- over D-leucine (or phenylalanine) was observed. No significant difference was seen when the spontaneous hydrolysis of 5′-[^{14}C] L-Ala-p-oligonucleotide *versus* 5′-[^{14}C] D-Ala-p-oligonucleotide was compared, either in the presence or absence of the bridging oligonucleotide. In addition, no significant difference in relative yields of L- *versus* D-aminoacyl- minihelix products was noted at 10, 20 or 30 min over the course of the reaction. Thus, chiral preference appears to occur during aminoacyl transfer from the 5′-phosphate to the minihelix. It might be noted that the mutual spatial orientation and distance between reacting molecular segments in the model system studied by Tamura and Schimmel could be different from a corresponding biological system, which might influence the observed ratio of selectivity.

Tamura and Schimmel also synthesised the aminoacyl phosphate oligonucleotide, bridging oligonucleotide and minihelix^{Ala}, which contain L-ribose (in contrast with natural D-ribose). Minihelix^{Ala}, bridging oligonucleotide, and either 5′-[^{14}C]-L-Ala-p-dT_6dA_2 or 5′-[^{14}C]-D-Ala-p-dT_6dA_2 (both containing L-deoxyribose) were combined and analysed for aminoacylation of minihelix^{Ala}. Formation of [^{14}C]-D-Ala minihelix was preferred over that of [^{14}C] L-Ala minihelix at a ratio of 1:3.6, about the reciprocal of that determined when we used RNA containing D-ribose. This result again points out the complementary heterochiral relationship between L-amino acid and D-sugar, which seems to play also a role in the aminoacylation reaction. The chiral-selectivity of the reaction with three different amino acids (alanine, leucine and phenylalanine) was 4-fold, although small, can lead to an overwhelming preference for an L-amino acid in a biological system.

In a subsequent study, Tamura and Schimmel [134] attempted to address whether the free amino group attached to the asymmetric α-carbon of the amino acid played a role in the chiral selectivity of aminoacylation. The aminoacylation reaction was performed with minihelix^{Ala}, bridging oligonucleotide and 5′-*N*-acetyl-[^{14}C]Ala-p-dT$_6$dA$_2$. It is pointed out that the free amino group (whether or not protonated) of amino acid as well as a free ribose hydroxyl are possible candidates to interact with a phosphate oxygen in the process of formation of the relevant transition state of the reaction. To address the question, the amino group of Ala was acetylated, and *N*-acetyl-L- or D-Ala-aminoacyl oligonucleotide was used for the aminoacylation reaction. Acetylation of Ala was performed with more than 70% of both L-[^{14}C]Ala and D-[^{14}C]Ala being acetylated. The ratio of the product formed (calculated from the band intensities of products resolved by gel electrophoresis) after 30 min at 0°C was 3.7:1 (Ac-L-Ala: Ac-D-Ala). This selectivity was similar to that for non-acetylated Ala, which was 1:4. These results suggest that, at least during the rate-determining step, the amino group of Ala does not make any hydrogen bonds with the phosphate oxygen of the terminal adenosine of the minihelix or with another H-bond acceptor located elsewhere in the complex.

Consideration of steric models of the base pairing at the position closest to the amino acid attachment site shows that a potential clash of the CH_3 of dT with the CH_3 of L-Ala is absent in the Watson–Crick dT: A pair [134]. While the CH_3 of D-Ala crowds this 3′-OH of A, the CH_3 of L-Ala is distal to the same 3′-OH. Based on such model building, a dT: G pair was introduced to create a potential clash of the CH_3 of L-Ala with that of dT. This substitution sharply reduced the yield of L-Ala-minihelix^{Ala} without altering production of D-Ala-minihelix^{Ala}. A suppression of the chiral-selective aminoacylation is noted and even somewhat reversed in favour of the D-Ala-minihelix^{Ala} product. Similarly, removal of the ring CH_3 through substituting at dU: G for a dT: G pair gave a structure in which chiral preference for L-Ala was retained, which is consistent with the possibility of a clash between the ring and the L-amino acid methyl groups. They also investigated the subtle effect of steric clash due to sugar ring puckering in the process of the selectivity. In the Watson–Crick dT: A pair, the potential clash of the CH_3 of dT with the CH_3 of L-Ala could be avoided through a 3′-endo pucker of dT. In contrast, conversion to the 2′-pucker could bring the CH_3 of dT close to the CH_3 of L-Ala. The NMR structure of a dT:dG base pair established a 2′-endo preference for the deoxyribose of dT. The distance between the 3′-O of dT and the 2-amino group of dG (which is 7.2 Å) could be bridged by a water molecule. A 3′-endo pucker preference can be created by making a ribose 2′-O-CH_3 substitution. Accordingly, a dT (2′-O-Me): G pair was introduced, and chiral selective aminoacylation in favour of the L-Ala product was observed. Also, to remove the capacity for making a water bridge between the 3′-O and a base that would stabilise the 2′-endo conformation, a dT: I (inosine) pair was also tested. This construct also showed the chiral preference for L-Ala. These results support the idea that the chiral preference for L-Ala in these constructs depends on avoiding a sugar-pucker sensitive steric clash between a pendant group of a base with the CH_3 of L-Ala.

Tamura and Schimel pointed out that the chiral preference can arise during the process of aminoacyl transfer from the 5′-phosphate of the oligonucleotide to the minihelix or from a difference in template (bridging oligonucleotide) hybridization efficiency between the L-amino acid and D-amino acid-poligonucleotides, rather than from a reaction within the ternary complex itself. The consequences of varying the concentration of the bridging

oligonucleotide are explored to determine whether the rate of aminoacylation was sensitive to its concentration and, at the same time, affected the ratio of L- to D-products. The amount of aminoacylation measured at four different time points was sensitive to the concentration of bridging oligonucleotide. However, at all time points and at all concentrations of the bridging oligonucleotide, the nearly 4-fold preference of L-Ala-minihelix^{Ala} to D-Ala-minihelix^{Ala} was observed. This result further supports the idea that chiral selectivity comes during aminoacyl transfer in the tripartite complex. The detailed work of Tamura and Schimmel indicates that an energetic difference of <1 kcal/mol in the rate-determining step of the transition state is sufficient to give the observed 4-fold preference for chiral specificity in the aminoacylation process. It may be noted that the ease of formation of a transition state in the model tripartite complex studied by the authors is more than the corresponding reaction within the active site of aminoacyl transferase. The reacting moieties in the latter case are surrounded by the active-site residues, which influence the progress of reaction in the cases of L- and D-reactant.

As mentioned in the beginning of this section, the size-based mechanism suggested in literature [114,115] is not capable of explaining the observed discrimination of the enantiomeric species of the cognate amino acid as the D- and L-enantiomers have identical total size. Neither acylation site nor the editing site would be able to discriminate the enantiomers if the size factor is essentially controlling the proofreading process. The chiral discrimination by AARS can be better understood in terms of the difference in electrostatic interactions (ionic, polar or hydrogen bonded) between AARS and amino acid as described in the following section.

5. Chiral discrimination in the amino acylation reaction in the aminoacyl transferase: computational studies

Thompson *et al.* [135] investigated the preference for acylation of L-Asp over D-Asp by Aspartyl-tRNA synthetase (AspRS), using detailed molecular dynamics simulations and considering the electrostatic interactions present in the system. The model system includes the synthetase, amino acid, ATP, co-bound ions and the solvent molecules. A 24 Å sphere of protein centred on the ligand, immersed in a 73 Å box of water with four sodium counterions is considered using CHARMM force field. It is pointed out that the proofreading of Asp is difficult for AspRS as it must protect not only against D-Asp, but against an 'inverted' orientation where the two substrate carboxylates are swapped. Inverted D-Asp binding gives a free energy 4.7 kcal/mol higher than L-Asp. Discrimination against D-Asp can be explained by unfavourable binding with the inverted D-Asp; binding is slightly better than D-Asp binding in the regular orientation. This raises a possibility that D-Asp may acylate tRNA with its side chain rather than its backbone carboxylate (at least partly). For both TyrRS and AspRS, a moderate binding free energy difference between the L- and D-amino acids is noted, which is in agreement with their known ability to misacylate their tRNAs. It is predicted that AspRS is strongly protected against inverted L-Asp binding. Based on component analysis, it is indicated that Coulomb interactions with the protein provide +13.1 kcal/mol in favour of the L-Asp geometry, offset by −6.2 kcal/mol from water. An additional +3.2 kcal/mol energy is contributed by van der Waals interactions giving a total free energy +10.4 kcal/mol in favour of the regular L-Asp binding geometry. Thus, less favourable van der Waals interactions for inverted L-Asp

contribute 31% of the overall effect, whereas Coulomb interactions contribute 69%. Co-binding of ATP and its three divalent cations does not affect binding specificity, contributing only −0.2 kcal/mol to the free energy. The weaker coordination of the displaced ligand ammonium to the flipping loop Glu171 prevents L-Asp from binding in an inverted geometry. The study points out that the networks of electrostatic interaction present in AARS is the major influence that protects AspRS against most binding errors.

In a recent work, Dutta Banik and Nandi [136] studied the chiral discrimination in the first step of aminoacylation reaction using ONIOM-based calculation. It is noted that during the reaction starting from the reactant state to form the product, the chiral discrimination can arise at least from the following factors: (1) During the formation of product, the amino acid moiety has to reorient and approach to form the adenylate from the free product state. The relative ease of the rotatory path for the approach of D-amino acid towards the ATP may be different from that of the L-amino acid. Their nanoscale separation is important for discrimination as it is known that discrimination is significant at such separation. (2) The transition state structure could be different for alteration of chirality, which can contribute to the chiral discrimination. Of course, the surrounding amino acids present near the active site of aminoacyl synthetase (of nanometre range) and their restricted orientation have influence on the discrimination.

In order to investigate that the relative ease of the rotatory path related to the approach of the L- and D-amino acid towards the ATP leading, the corresponding orientation-dependent interaction profile is studied. The relative orientation of histidine, ATP and the surrounding residues is different in the crystal structures of the reactant and the product, respectively. The reacting moieties should undergo orientational rearrangement, which can contribute to the discrimination [136]. The crystal structure of the oligomeric complex of histidyl-tRNA synthetase (HisRS) from *E. coli* complexed with ATP and histidinol and histidyl-adenylate [137] is used for the computation. The active site of the reactant consists of histidine, ATP and the active site of product consists of histidyl-adenylate as well as the surrounding residues of histidyl-tRNA synthetase. The surrounding residues enclose the His and the ATP within a cavity of dimension in nanometre range. An image of the cavity is shown in Figure 19(a). The His and the ATP moiety are enclosed within this restricted space. The surrounding residues like Gln-83, Arg-113, Arg-121, Gln-127 Glu-131, Arg-259 and Tyr-264 are included in the computation. Comparing the reactant and the product geometry, a change in orientation of the amino acid moiety relative to the ATP occurs in a plane containing the α-phosphorus atom of ATP, carboxyl carbon of amino acid, chiral carbon and is nearly perpendicular to the plane containing the imidazole ring of the histidine moiety. The relative ease of the rotatory path related to the approach of the L- and D-amino acid towards the ATP leading to the corresponding product is studied from the variation of interaction energy. The amino acid is present as histidinol in the crystal structure obtained in the experiment as it is present in the form of an inhibitor. The structure of the amino acid is modified from histidinol to histidine with its carboxylic acid group to perform the reaction.

Electrostatic interaction plays an important role in the first step of aminoacylation [138]. The crystal structure ATP contains four negative charges on oxygen atoms attached to the α, β and γ phosphate groups, which are coupled with two bivalent metal ions. Two models are considered. In the first model (model I) of the active site, the metal

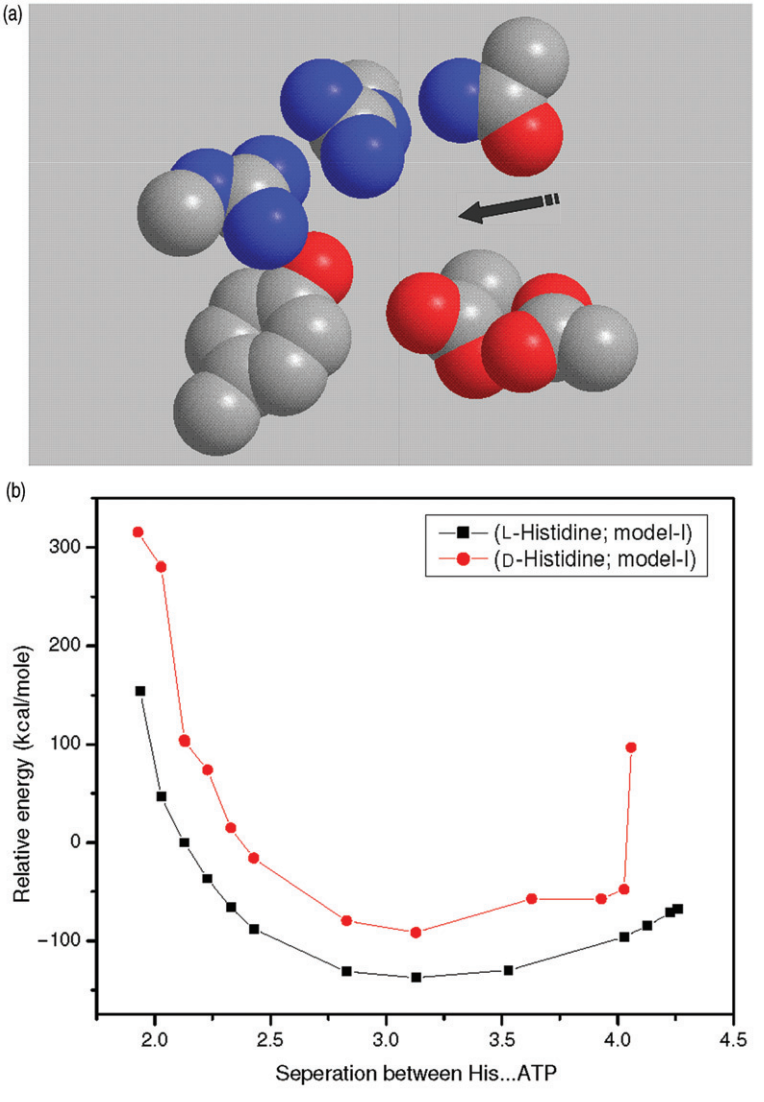

Figure 19. [Colour online] (a) Image of the cavity (indicated by the bold arrow) enclosing the His and ATP within the active site of reactant state (1KMN.PDB) The His and ATP are omitted for clarity (b) The variation of the relative intermolecular energy (relative to the energy in the model based on crystal structure expressed in kcal/mol) as a function distance of the L- and D-amino acid moiety measured between the oxygen of the carboxylic group of the His moiety and the α-phosphorus atom of ATP (in Å) studied in model I. The Gln-83, Arg-113, Gln-127, Glu-131, Arg-259 and Tyr-264 are present as surrounding residues in the model (reprinted from reference [136] with permission from the Elsevier. © Elsevier).

ions are removed and the charged oxygen atoms attached to the β and γ phosphate groups are neutralised as hydroxyl groups. The surrounding residues include Gln-83, Arg-113, Gln-127, Glu-131, Arg-259 and Tyr-264. In order to study the effect of the electrostatic interaction on the chiral discrimination, the charge over the amino group of $-NH_3^+$ and

charge of the ATP are removed in a second model (model II). A two-layered ONIOM model is used (*ab initio* HF: semiempirical PM3 level of theory). The *ab initio* level of theory (HF/6-31G) is applied to histidine and ATP moieties, which are directly involved in the reaction, and semi-empirical level of theory (PM3) is applied to all the remaining atoms that are anchoring residues in the model of active-site region.

The variation of intermolecular energy of the L- and D-amino acid moiety as a function of distance measured between the oxygen of the carboxylic group of the His moiety and the α-phosphrous atom of ATP (in Å) is studied in model I and is shown in Figure 19(b). The result shows that the interaction energy rises as the His-substrate and ATP separation shortens during the mutual approach of the His and the ATP moiety in the cavity and can be understood from the short-range repulsion between the reacting species. The energy again rises at larger separation due to the repulsive interaction between the His and its neighbouring residues present as well as the ATP and its neighbouring residues present in aminoacyl synthetase. However, the corresponding variation in the separation is more restricted and unfavourable for the D-His compared to L-His as shown in the Figure 19(b), which is a signature of chiral discrimination. The restriction of the degrees of freedom enhances the chiral discrimination.

The change in intermolecular energy as a function of mutual orientation of the L- and D-amino acid moiety relative to the ATP as occurs in a plane containing the α-phosphorus atom of ATP, carboxyl carbon of amino acid, chiral carbon (nearly perpendicular to the plane containing the imidazole ring of the histidine moiety) is shown in Figure 20. The result shows that the reorientation required for going to the product state for L-amino acid is without any significant energy barrier and its approach is favoured relative to the same for the corresponding D-amino acid. It may be noted that the conformational energy differences between the D or L molecules themselves are negligibly small (0.60 kcal/mol computed at the level of HF/6-31G) and the observed difference in the intermolecular potential is not due to any conformational difference but arising from interaction between the D-enantiomer with the neighbouring moieties. The result indicates that the incorporation of the D-form as an adenylate in the first step is strongly unfavoured. The difference is ~100 kcal/mol to ~200 kcal/mol at the level of theory considered. The unfavourable interaction of D-enantiomer is partly due to the unfavourable electrostatic interaction of the amino group of histidine with the phosphate groups of ATP as well as a reduction of a favourable interaction between the amino group of histidine and Glu-83.

The variation of intermolecular energy as a function of the orientation of the L- and D-amino acid moiety relative to the ATP as occurs in a plane containing the α-phosphorus atom of ATP, carboxyl carbon of amino acid, chiral carbon (nearly perpendicular to the plane containing the imidazole ring of the histidine moiety) as studied in model II (where the charge over the amino group of $-NH_3^+$ of L-histidine and D-histidine and charge of the α-phosphate are removed) is shown in Figure 21. The unfavourable nature of the interaction in the case of D-enantiomer is diminished in part when the charges are reduced in the model II, relative to the model I. This can be concluded from the reduction in the unfavourable interaction energy of D-His in the range of mutual orientation of -5° to -15°, as shown in Figure 21, relative to the same range of orientation when the charges over the His and ATP are present as shown in Figure 20.

The effect of the surrounding residues on the chiral discrimination is studied by removing Tyr-264. In the case of model I containing L-His, the hydrogen bonding

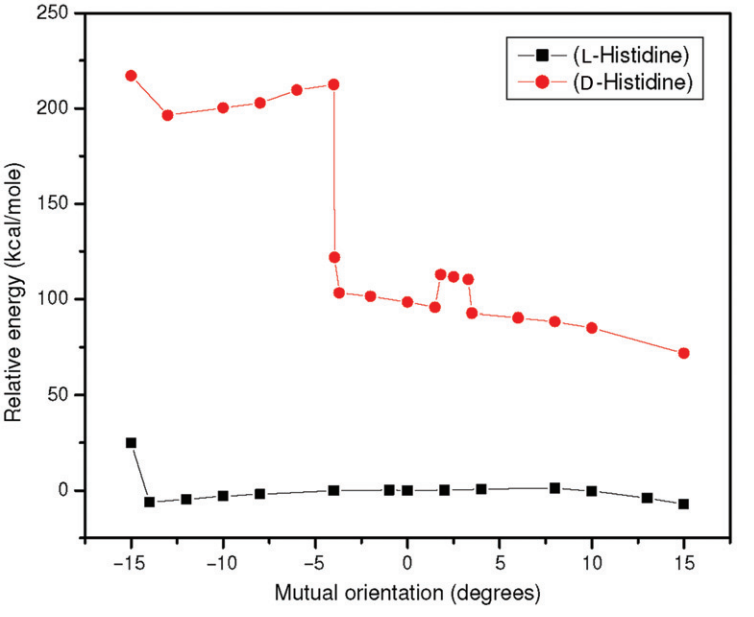

Figure 20. [Colour online] The variation of the relative intermolecular energy (relative to the energy in the model based on crystal structure expressed in kcal/mol) as a function orientation of the L- and D- amino acid moiety relative to the ATP as occurs in a plane containing the α-phosphorus atom of ATP, carboxyl carbon of amino acid, chiral carbon (nearly perpendicular to the plane containing the imidazole ring of the histidine moiety) studied in model I. The Gln-83, Arg-113, Gln-127, Glu-131, Arg-259 and Tyr-264 are present as surrounding residues in the model I (reprinted from reference [136] with permission from the Elsevier. © Elsevier).

interaction between the nitrogen atom of the imidazole group of the histidine residue and the hydroxyl group of the aromatic ring of the Tyr-264 is lost and the energy of the system becomes unfavourable as noted in Figure 22. In the case of D-His, in addition to the hydrogen bonding interaction between the nitrogen atom of the imidazole group of the histidine residue and the hydroxyl group of the aromatic ring of the Tyr-264, favourable electrostatic interaction between the amino group of the His residue and the hydroxyl group of the aromatic ring of the Tyr-264 is present. Removal of the Tyr-264 in the model of D-His further enhances the unfavourable nature of the rotatory path compared to the case when Tyr-264 is removed in the L-model. The result points out that the surrounding residues of the synthetase not only stabilise the reacting moieties in the case of synthetase with natural L-substrate but also play a significant role in discriminating D-enantiomer of the cognate amino acid.

The conclusion that the surrounding residue Tyr-264 influences the discrimination of the D-enantiomer of the cognate His substrate can be confirmed from Figure 23. The variation in intermolecular energy as a function of mutual orientation is studied in this plot for model I and model II for D-His only. The approach of D-His is unfavourable compared to L-His for the range of mutual orientation beyond -5° as the Tyr-264 loses its favourable electrostatic interaction with His when it is present in the stereochemical arrangement corresponding to the D-form. The unfavourable interaction diminished

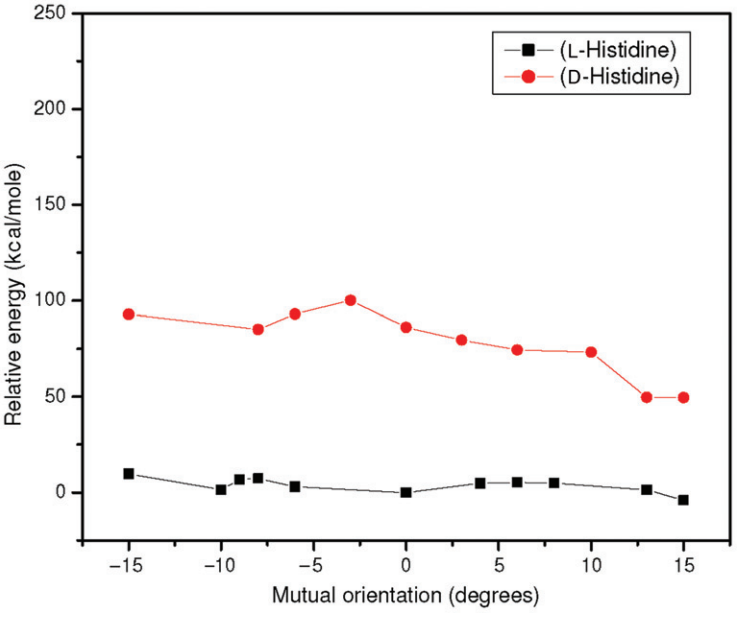

Figure 21. [Colour online] The variation of the relative intermolecular energy (relative to the energy in the model based on crystal structure expressed in kcal/mol) as a function orientation of the L- and D-amino acid moiety relative to the ATP as occurs in a plane containing the α-phosphorus atom of ATP, carboxyl carbon of amino acid, chiral carbon (nearly perpendicular to the plane containing the imidazole ring of the histidine moiety). The Gln-83, Arg-113, Gln-127, Glu-131, Arg-259 and Tyr-264 are present as surrounding residues in the model II (reprinted from reference [136] with permission from the Elsevier. © Elsevier).

drastically as the electrostatic interaction is reduced in model II by removing the charges over NH_3^+ and the α-phosphate group of ATP as present in model I. Further, the removal of Tyr-264 also does not exhibit any unfavourable interaction (noted in model I) in the absence of electrostatic interaction. This strongly indicates that the electrostatic interactions of the substrate with the surrounding residues are vital in discriminating the D-enantiomer of the cognate amino acid and the chiral discrimination vanishes when such interaction is lost.

A look into the transition state of L-His and ATP in model I, shows that the stability of the transition state geometry depends on the favourable electrostatic interaction between the Arg-259 and oxygen of the α-phosphate group of ATP as well as the Glu-83 and NH_3^+ group of the L-His moiety, as shown in Figure 24(a), However, the interaction of the Glu-83 and NH_3^+ group of the L-His moiety is lost when the chirality of the His substrate is changed to D- as shown in a model (Figure 24b) built from the transition state obtained in the case of L-His (Figure 24a) by exchanging the groups at α-carbon atom of His. The loss of the interaction is noted in as the corresponding groups are moved away from each other and the corresponding transition state of the D-His is relatively destabilised compared to the L-enantiomer.

Several factors are noted to be responsible for the discrimination and explain the high level of stereospecificity of the process. The factors can be listed as follows: (1) The chirality

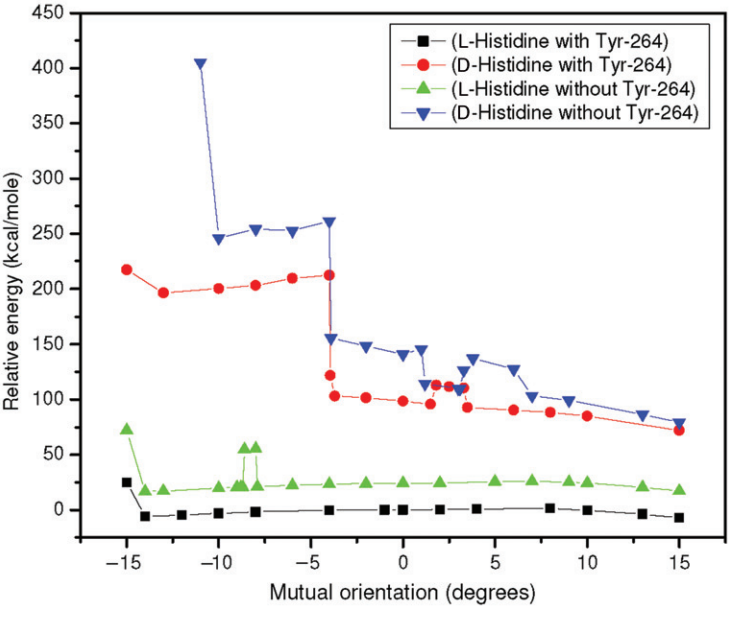

Figure 22. [Colour online] The effect of the Tyr-264 as a surrounding residue on the variation of the relative intermolecular energy (relative to the energy in the model based on crystal structure expressed in kcal/mol) as a function orientation of the L- and D-amino acid moiety relative to the ATP as occurs in a plane containing the α-phosphorus atom of ATP, carboxyl carbon of amino acid, chiral carbon (nearly perpendicular to the plane containing the imidazole ring of the histidine moiety). The Gln-83, Arg-113, Gln-127, Glu-131 and Arg-259 residues are also present (reprinted from reference [136] with permission from Elsevier. © Elsevier).

of the amino acid of the substrate and its (principally) electrostatic interaction with the ATP. The distance and orientational changes involved in the approach of D-amino acid towards the ATP is unfavourable. The charge distribution is important for discrimination. Removal of the charges in the model drastically reduces the discrimination. (2) Restricted nature of the mutual orientation within the cavity of the active site where the His and ATP are located during the change in orientation for the approach to form the adenylate make the resultant interaction profile as different for L-His and D-His exhibiting discrimination. (3) The analysis of the transition state structure revealed that alteration of the chirality of the His destabilises the transition state by removing favourable electrostatic interaction between the Glu-83 and NH_3^+ group of the His substrate. (4) The proximity of the surrounding residues present in the active site of the synthetase with the His and ATP (of nanometre range) and their restricted orientation have an influence discrimination. These factors cause the discrimination in amino acylation to be accurate.

6. Chiral discrimination and chirality-dependent interactions in biological cavities involving amino acids and peptides

Chirality is present in the protein structural hierarchy at the primary (amino acids, except glycine), secondary (α-helices, β-sheets), tertiary (domains and subdomains) and

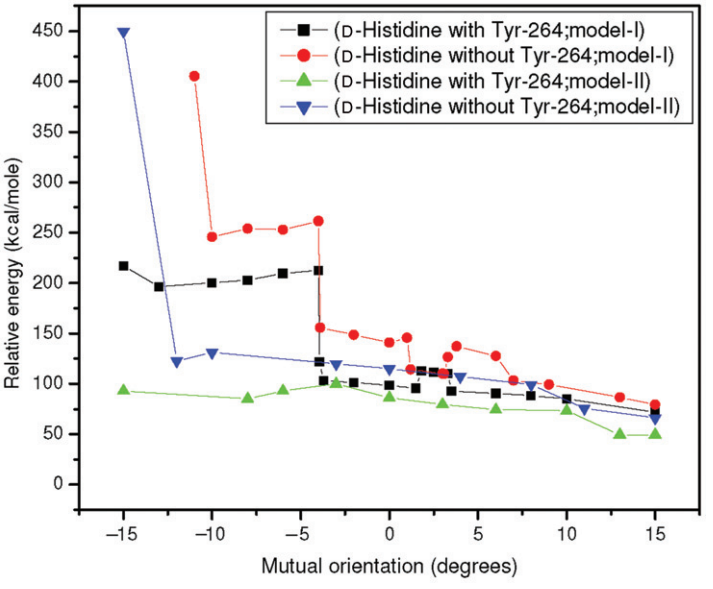

Figure 23. [Colour online] The effect of the Tyr-264 as a surrounding residue on the variation of the relative intermolecular energy (relative to the energy in the model based on crystal structure expressed in kcal/mol) as a function orientation of the D-amino acid moiety relative to the ATP as occurs in a plane containing the α-phosphorus atom of ATP, carboxyl carbon of amino acid, chiral carbon (nearly perpendicular to the plane containing the imidazole ring of the histidine moiety) for models I and II, respectively (models differ in the charge distribution). The Gln-83, Arg-113, Gln-127, Glu-131 and Arg-259 residues are also present (reprinted from reference [136] with permission from the Elsevier. © Elsevier).

quaternary structures. It is expected that these structural features are related to function, for example, in the process of interaction with an external ligand molecule, which is not covalently attached to the biological chiral structure (not an integral part of the protein structure). In a recent study, it was shown that the chirality of the helix (which depends on the spatial arrangement of residues) has a significant influence on the orientation-dependent interaction with the chiral ligand [34]. The related discrimination is shown to arise from the helicity (secondary level) and not from the chirality of the primary level subunits. Helical chirality is present in many important biological structures like protein, nucleic acid and lipid systems. It is expected that chiral discrimination will be observed as the proteins and nucleic acids both have chirality in different levels of their structure.

In a series of studies Gabbay and co-workers studied the discrimination related to amino acid and nucleic acid interaction. Gabbay and Kleinman have shown that the L enantiomers of the amino acid amides of the general structure $^{+}NH_3CHRCONHCH_2CH_2 - NMe_2H^{+}2Br^{-}$, interact more strongly with nucleic acid helices than the corresponding D enantiomers [139–142]. Subsequently, the effect of diamino acids of the general structure, $^{+}NH_3CH(CO_2^{-})(CH_2)_nN^{+}H_3Cl^{-}$ and lysyl dipeptides $^{+}NH_3CH((CH_2)_4N^{+}H_3)CONHCHRCO_2^{-}Br^{-}$ on the melting temperature of polyriboinosinic–polyribocytidylic acids (rI–rC), polyriboadenylic–polyribouridylic acids

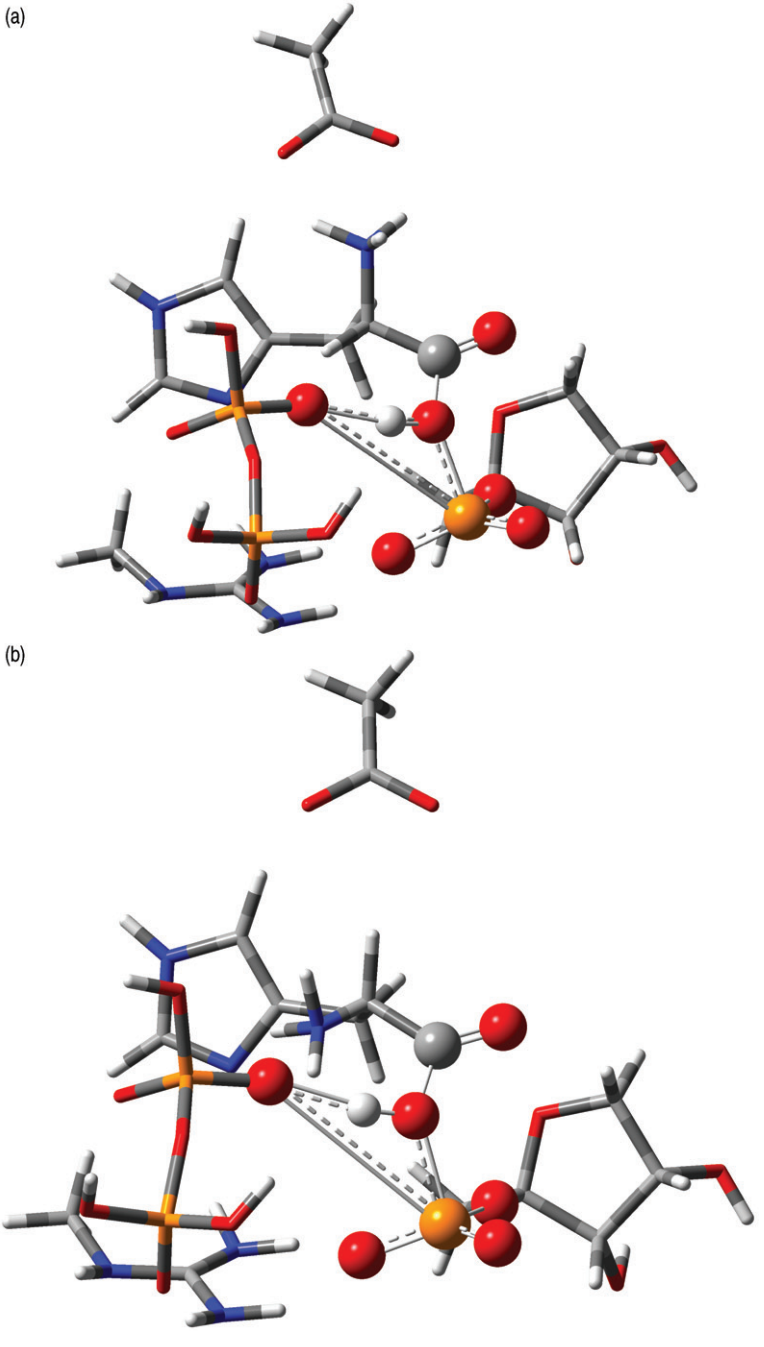

Figure 24. [Colour online] (a) Transition state geometry for the first step of the aminoacylation reaction with L-His at the ONIOM (HF/6-31G: PM3) level of theory (b) Model of the corresponding geometry when D-His is present as substrate (constructed from the geometry shown for L-isomer) (reprinted from reference [136] with permission from the Elsevier. © Elsevier).

(rA–rU) and calf thymus DNA is studied [143]. There is very little difference in the degree of stabilisation of polyriboadenylic–polyribouridylic (rA–rU) and calf thymus DNA helices by the L and DL mixture of the diamino acids. However, there is a very large difference in the degree of stabilisation of the polyriboinosinic–polyribocytidylic helix. The degree of stabilisation of the helices by the diamino acids is considerably lower than the diammonium salts, $^{+}NH_3^{-}(CH_2)_nN^{+}H_3 \cdot 2Br^{-}$, due to the presence of the negatively charged carboxyl group. The effect of the neighbouring negatively charged group is seen dramatically in the lysine system. For example, approximately the same degrees of stabilisation of the rI–rC and rA–rU helices are obtained by the lysyl dipeptides at one-tenth of the concentration of lysine. The LL-lysyl dieptides stabilise the nucleic acid helices to a greater degree than the corresponding DDlysyl dipeptides. Although the difference in the degree of stabilisation of calf thymus DNA by the LL and DD enantiomers is not substantial, it is still outside the experimental error.

Subsequent studies of the interaction specificities of L-lysyl-L-phenylalaninamide and the diastereomeric dipeptide amide, L-lysyl-D-phenylalaninamide, with salmon sperm DNA reveal distinct differences in the binding site of the aromatic ring of the phenylalanine residue [144]. The results of ^1H nuclear magnetic resonance, spin-lattice relaxation rates, viscometric and flow dichroism studies indicate that the aromatic ring of L-lysyl-L-phenylalaninamide is partially inserted between base pairs of DNA whereas the aromatic ring of L-lysyl-D-phenylalaninamide points outward towards the solution. The terminal L-lysyl residue presumably stereospecifically interacts with DNA helix thus dictating the positioning of the aromatic ring of the C-terminal phenylalanine residue. It is indicated that the peptides may bind to DNA via an intercalated mechanism. A wedge-type partial insertion is suggested. Since it has been previously shown by Gabbay and co-workers that L- and D-phenylalaninamide interact similarly to DNA, it is concluded that the *N*-terminal L-lysyl residue binds stereospecifically to DNA and dictates the positioning of the aromatic ring of the C-terminal phenylalanine residue.

Chiral discrimination of the *N*-acetyl-L-phenyl alanine and *N*-acetyl-D-phenyl alanine in the toroidal cavity of β-cyclodextrin is studied [145]. At low temperature, the distribution of guest molecule can be located, which is not possible at room temperature and is disordered. The β-cyclodextrin complex crytal lattice is chiral and can lead to the discrimination of the packing arrangement of the enantiomeric guest molecule. While the restricted environment of the cavity of the β-cyclodextrin is expected to enhance the discrimination, further analysis concerning the temperature dependence of the discrimination is required.

The above studies indicate that the grooves and cavities of DNA and cyclodextrin are capable of discriminating amino acid. It is expected that the nanoscale intermolecular separation between the ligand and the recognition site in these cases might play a role. The restricted orientation of the amino acids near the groove of DNA or within the cavity of the cyclodextrin might also play a role. However, more molecular studies are needed to confirm this conjecture in such systems. The understanding might be useful in intercalation of enantiomeric drug as many drugs target DNA. Since cyclodextrin cavities are used for drug encapsulation, the study of chiral discrimination in cyclodextrin is also important.

7. Concluding remarks

In Section 1, a few questions pertaining to the chiral discrimination in biological systems have been raised, namely, about the influence of the chirality of the amino acids and sugars themselves and their mutual influence on peptide synthesis and amino acylation reaction. It is pointed out that the underlying mechanism of the retention of enantiopurity and the fidelity of the discrimination is now beginning to emerge. Another aspect of the present review is about the effect of the confinement by the biological nanospace on the chiral discrimination exhibited by these reactions. In the following, we briefly summarise these influences revealed by experimental and computational studies in Sections 2–6.

Experimental studies on peptide synthesis have conclusively shown that it is impossible to incorporate D-amino acid into proteins without modifying the chemical structure of the PTC of naturally occurring tRNA. However, it is possible to perform the formation of a D–L peptide bond in the model or modified systems. A clear homochiral preference is noted favouring L-amino acid incorporation. Computational studies (combined quantum mechanical/molecular mechanical calculations) show that the chiral discrimination is not only driven by the chirality of the A- and P-terminals but is also due to the influence of the chirality of the D-sugar ring as well as the confinement by the surrounding bases of the PTC. Several factors are noted to be responsible for discrimination and explain the high level of stereospecificity of the process. The chirality of the amino acids at A- and P-terminals has significant influence on the discrimination. The rotatory path for the approach of D-amino acid towards the L-terminal is unfavourable due to steric hindrance between the terminals themselves. The nanoscale separation of these terminals is important for the discrimination and, at larger separation, discrimination is lost. The restricted nature of the mutual orientation between the terminals during the rotatory path for approach to form the peptide bond makes the resultant interaction profile different for L–L and D–L pair exhibiting discrimination. Favourable influence of the natural chirality (D-form) of the sugar ring for long-length scale organisation is also noted. Alteration of the chirality of the sugar ring is unfavourable as it requires large structural rearrangements of tRNA. The D-sugar ring favourably influences the rotatory path for the approach of the A- and P-terminals to form the peptide bond. The removal of the sugar ring makes the rotatory path as unfavourable, which indicates that the interaction of the D-sugar with the L-amino acid is more favourable than other homopair or heteropair combinations of sugar–amino acid chiralities. The stereochemistry at the 2′ centre of the D-sugar is vital as it catalyses the peptide bond formation by making proper placement of the OH group, which is involved in the catalysis. The analysis of the transition state structure revealed that alteration and removal of the chirality of the 2′ centre destabilise the transition state and make the formation of a peptide bond unfavourable. The nanoscale proximity of some of the surrounding bases present in PTC with the A- and P-terminals and their restricted orientation have influence on the discrimination. Thus, it is revealed that multiple factors drive the discrimination in peptide synthesis and control the precision and retention of the biological homochirality.

The aminoacylation reaction involves chiral amino acids and sugars and occurs within the active site of aminoacyl transferase which is composed of chiral amino acids rather than the achiral surrounding residues (bases) present in PTC. These surrounding chiral amino acids are located within a nanoscale distance. Thus, it is not surprising that the aminoacylation reaction exhibits stringent chiral discrimination. Other than the factors

noted to be important for chiral discrimination in peptide synthesis (e.g. the chiralities of the substrates, surrounding amino acids in active site, their confinement and proximity in the cavity in a nanoscale range), a network of electrostatic interaction present in the active site is suggested to play a significant role here. The charge distribution in and around the active site is important for discrimination. Reduction of the charges drastically reduces the discrimination. The electrostatic interaction of the substrate and the ATP is noted to be important. The distance and orientational changes involved in the approach of D-amino acid towards the ATP is found to be unfavourable relative to the L-enantiomer. The restricted nature of the mutual orientation within the cavity of the active site where the amino acid and ATP are located during the change in orientation for the approach to form the adenylate make the resultant interaction profile different for L- and D-amino acid exhibiting discrimination. A look into the transition state structure revealed that alteration of the chirality of the amino acid destabilises the transition state as well by removing favourable electrostatic interaction between the surrounding residue present in the active site and the amino acid substrate. The proximity of the surrounding residues present in the active site of the synthetase with the amino acid and ATP (of nanometre range) and their restricted orientation have an influence on discrimination. These factors cause the discrimination in amino acylation to be stringent. Chiral discrimination in the interactions involving amino acids and peptides in the biological cavities of nucleic acid, cyclodextrin are also briefly reviewed.

While the foregoing conclusions provide molecular understanding of the retention of biological homochirality and the related questions raised in Section 1, the understanding might be useful in following the principles of chiral molecular recognition in diverse systems. It is possible to extend the principles towards the material systems in order to gain control over the technique of nanofabrication of designer materials. Specific structures using chiral subunits (or achiral subunits in some cases) can be developed, which might have improved function. Here, we mention a few studies where the influence of the chirality and discrimination may be noted while building diverse nanomaterials. Future studies of the exploration of the role of molecular chirality and confinement might be interesting and useful.

Numerous nanomaterials are designed through the process of self-assembly [146,147]. In a recent study, excellent control of enantioselectivity of amino acid recognition is achieved by cholesterol armed cyclen monolayer at the air–water interface [148]. The host system is composed of cholesterol, which is chiral, and the Na^+ complex of cyclen has helical structure. Consequently, the system has multiple levels of chirality and exhibits significant enantioselectivity with leucine and valine. When leucine or valine was added to the subphase, the isotherms were shifted to larger molecular areas with increasing amino acid concentration. The isotherms in the presence of aqueous D-leucine are shifted to larger molecular areas than the same in the presence of aqueous L-leucine of the same concentration exhibiting discrimination. In contrast, the difference between the isotherms on aqueous L- and D-valines is insignificant. While these results suggest a greater and negligible enantioselectivity for leucine and valine, significant chiral discrimination is also noted for valine when the binding constant (K) is studied. The K values of D-leucine are always greater than those of L-leucine, indicating that the monolayers have a stronger interaction with D-leucine. Conversely, the values of L-valine are smaller than those of D-valine at low surface pressure but exceed them at 22–23 $mN\,m^{-1}$. The result shows that

the chiral discrimination and concomitant recognition in monolayers with valine changes from the D- to L-form upon compression. The result shows for the first time that the subtle difference in the chemical structure between leucine and valine can be distinguished by the dynamic process of monolayer formation. The multilevel chirality of the host, dissymmetry of air–water interface and the confinement in the nanoscale proximity of aggregate seem to have a substantial influence on the recognition observed. The result shows that it is possible to construct nanoscale assemblies by which one can gain better control of enantioselectivity.

We have noted in this review that, when confined (with a restricted degrees of freedom), achiral molecular segments such as nucleobases can influence the discrimination in biological systems. It is noted in biomimetic models that achiral shapes arranged in a chiral (helical) way might have a dissymmetric interaction profile with a ligand (a signature of chiral discrimination) [34]. The synthetic molecule, 2-(heptadecyl) naphtha-[2,3]-imidazole, was found to form a bilayer film on a water surface. The *in situ* coordinated Langmuir–Blodgett (LB) films composed of the molecule and Ag^{+} ion showed chirality due to the formation of a helical coordination polymer where the naphtha-[2,3]-imidazole group distorted in a certain degree along the polymer backbone. Notably, both ligand and metal ions are achiral [149]. The coordination and the interaction between the naphtha [2,3] imidazole rings play an important role in forming the chiral LB films. The results give important clues to the design and fabrication of chiral molecular assemblies from achiral molecules.

The importance of the controlled fabrication of nanometre-scale objects, which is a central issue in current science and technology, has been recently discussed in an authoritative review [150]. Diverse materials are designed by self-assembly which have technical utility or might have potential in that direction. In a recent novel study, inorganic nanorods are used to develop optically driven nanorotors. The principle of this nanorotor is dependent on the non-zero chirality of the nanorod structure [151]. The inherent textural irregularities or morphological asymmetries of the nanorods give rise to the torque under the radiation pressure. The presence of non-zero chirality (arising from a small surface irregularity or extrusion) is sufficient to produce enough torque for reasonable rotational speed. As the extrusion is not symmetric about a plane passing through the z-axis, it will provide a net chirality of the nanorod structure. Therefore, the radiation pressure force will generate a non-zero torque on the nanorod. The controllability, simplicity and flexibility of the rotational motion of these rotors suggest that this scheme can be applied universally to devise easy-to-use optically driven nanorotors. The availability of inorganic nanorods bearing the desired size and chirality would favour the present scheme to design nanorotors with predictable rotational speeds. It might be possible that nanostructures and nanomachines with controllability can be constructed by tuning the chirality of the constituent nanomaterial. Exploiting nanospaces by the confinement of the immobilised chiral catalysts is found to be useful in asymmetric catalysis, which is an extremely important field of research in general [152]. The study of the role of the confined chiral moieties in the process of biological catalysis and the importance of the effect of the spatial restrictions imposed by the catalytic systems might be useful to explore the development of novel catalysts with enhanced function.

The study of chiral discrimination in the confined spaces has biomedical prospect. A large proportion of clinically useful antibiotics exert their effects by blocking protein

synthesis at PTC in ribosome [153]. Understanding the recognition process at PTC has technological relevance for new drug design. This biomedical target is particularly important considering the problem of the recurrent development of antibiotic resistance. It is discussed in the present review that the modification of the structure of PTC can lead to alteration of chiral selectivity [94,99,101]. Mutation of the PTC (a nanoflask) can lead to the achievement of controlled protein synthesis. More molecular studies are necessary to explore the recognition event in such cavities. A further point is that while the works described in the present review principally refers to the discrimination related to the thermodynamically stable state, the dynamical aspects of discrimination is also interesting. Confinement is already known to have important influence on dynamics [154]. The dynamics of the biological active sites and their influence on the confined chiral molecules would be interesting to explore and might reveal new aspects of chiral recognition in biology and medicine.

In the present review, some of the issues concerning the principles behind nature's technique in building the functional biological molecules, retention of their chiral structure and replication of these structures through evolution as well as the accurate performance of the corresponding life processes have been discussed. Combining these principles with the technological advancement already made might lead to the possible development of new synthetic architecture with desired functionality. The basic units of known materials of technological interests such as diverse polymers, crystals, liquid crystals and gels are rather simple in structure. Biological functional architectures are much more sophisticated. Nature has always been superior in designing the world through molecules on which the very existence of life depends. The immensely efficient and orchestrated synthesis of myriads of biomolecules uses biophysical principles to achieve this. The present review indicates that the confinement of biomolecules in a nanoscale dimension and their chirality is utilised in biosynthetic reactions to enhance fidelity. Thus, gaining the control over the methods of confinement of chiral moieties in a nanospace has vast potential in building up newer functional structures with desired physico-chemical characteristics.

Acknowledgements

The works by the author's laboratory described in this review are supported by the Department of Science and Technology, Government of India. The author thanks Mr K. Thirumoorthy and Ms S. Dutta Banik for the computational work and help in preparation of the manuscript.

References

[1] B. Testa, *Principles of Organic Stereochemistry* (Dekker, New York, 1979).
[2] E. L. Eliel, S. H. Wilen, and L. N. Mander, *Stereochemistry of Organic Compounds* (Wiley, New York, 1994).
[3] J. M. Berg, J. L. Tymoczko, and L. Stryer, *Biochemistry* (W.H. Freeman & Co., New York, 2002), pp. 41–43.
[4] S. F. Mason and G. E. Tranter, Mol. Phys. **53**, 1091 (1984).
[5] S. F. Mason and G. E. Tranter, Proc. Roy. Soc. London A **397**, 45 (1985).
[6] N. Nandi, D. Vollhardt, and G. Brezesinski, J. Phys. Chem. B **108**, 327 (2004).
[7] D. Andelman, J. Am. Chem. Soc. **111**, 6536 (1989).

[8] D. Andelman and H. Orland, J. Am. Chem. Soc. **115**, 12322 (1993).
[9] N. Nandi and D. Vollhardt, Chem. Rev. **103**, 4033 (2003).
[10] G. Guerra, L. Cavallo and P. Corradini, in *Materials Chirality*: *Volume 24 of Topics in Stereochemistry*, edited by M. M. Green, R. J. M. Nolte, E. W. Meijer, S. E. Denmark and J. Siegel, Series (Wiley Interscience, John Wiley & Sons, New York, NY, 2003), pp. 1–69.
[11] C. D. Rosa, in *Materials Chirality: Volume 24 of Topics in Stereochemistry*, edited by M. M. Green, R. J. M. Nolte, E. W. Meijer, S. E. Denmark and J. Siegel, Series (Wiley Interscience, John Wiley & Sons, New York, NY, 2003), pp. 71–155.
[12] Y. Okamoto, E. Yashima and C. Yamamoto, in *Materials Chirality: Volume 24 of Topics in Stereochemistry*, edited by M. M. Green, R. J. M. Nolte, E. W. Meijer, S. E. Denmark and J. Siegel, Series (Wiley Interscience, John Wiley & Sons, New York, NY, 2003), pp. 157–207.
[13] M. Fujiki, H. Nakashima, S. Toyoda and J. R. Koe, in *Materials Chirality: Volume 24 of Topics in Stereochemistry*, edited by M. M. Green, R. J. M. Nolte, E. W. Meijer, S. E. Denmark and J. Siegel, Series (Wiley Interscience, John Wiley & Sons, New York, NY, 2003), pp. 209–279.
[14] M. M. Green, K. Cheon, S. Yang, J. Park, S. Swansburg, and W. Liu., Acc. Chem. Res. **34**, 672 (2001).
[15] C. Chothia, T. Hubbard, S. Brenner, H. Barns, and A. Murzin, Annu. Rev. Biophys. Biomol. Struct. **26**, 597 (1997).
[16] N. Nandi and B. Bagchi, J. Am. Chem. Soc. **118**, 11208 (1996).
[17] N. Nandi and B. Bagchi, J. Phys. Chem. A **101**, 1343 (1997).
[18] (a) D. Berthier, T. Buffeteau, J.-M. Léger, R. Oda, and I. Huc, J. Am. Chem. Soc. **124**, 13486 (2002); (b) H. Jiang, C. Dolain, J.-M. Léger, H. Gornitzka, and I. Huc, J. Am. Chem. Soc. **126**, 1034 (2004); (c) C. Dolain, J.-M. Léger, N. Delsuc, P. Guionneau, and I. Huc, J. Am. Chem. Soc. **127**, 12943 (2005); (d) A. Brizard, R. Oda, and I. Huc, Top. Curr. Chem. **266**, 167 (2005); (e) V. Maurizot, C. Dolain, and I. Huc, Eur. J. Org. Chem. **7**, 1293 (2005).
[19] N. Nandi and D. Vollhardt, Thin Solid Films **433**, 12 (2003).
[20] N. Nandi, D. Vollhardt, in *Bottoms up Nanofabrication; Supramolecules, Self Assemblies and Organized Films*, edited by K. Ariga and H. S. Nalwa (American Scientific Publishers, Valencia, CA, 2006), Vol. 1.
[21] N. Nandi and D. Vollhardt, Acc. Chem. Res. **40**, 351 (2007).
[22] N. Nandi and D. Vollhardt, Curr. Opin. Colloid Surf. **13**, 40 (2008).
[23] (a) L. Brunsveld, E. W. Meijer, A. E. Rowan and R. J. M. Nolte, in *Materials Chirality: Volume 24 of Topics in Stereochemistry*, edited by M. M. Green, R. J. M. Nolte, E. W. Meijer, S. E. Denmark and J. Siegel, Series (Wiley Interscience, John Wiley & Sons, New York, NY, 2003), pp. 373–455; (b) D. M. Walba in *Materials Chirality: Volume 24 of Topics in Stereochemistry*, edited by M. M. Green, R. J. M. Nolte, E. W. Meijer, S. E. Denmark and J. Siegel, Series (Wiley Interscience, John Wiley & Sons, New York, NY, 2003), pp. 457–518.
[24] G. M. Maggiora, B. Mao, K. C. Chou in *New Developments in Molecular Chirality* edited by P. G. Mezey (Kluwer Academic Publishers, Norwell, MA, 1991), Vol. 93.
[25] R. I. Dima and D. Thirumalai, J. Phys. Chem. B **108**, 6564 (2004).
[26] R. Hegstrom and D. K. Kondepudi, Sci. Am. **262**, 108 (1990).
[27] R. Janoschek, editor, *Chirality – From Weak Boson to the Alpha-Helix* (Springer-Verlag, New York, 1991).
[28] D. K. Kondepudi and D. J. Durand, Chirality **13**, 351 (2001).
[29] G. Palyi, C. Zucchi, and L. Caglioti, in *Advances in Biochirality*, edited by G. Palyi, C. Zucchi, and L. Caglioti (Elsevier, Oxford, 1999), pp. 3–12.
[30] D. K. Kondepudi, in *Progress in Biological Chirality*, edited by G. Palyi (Elsevier, Oxford, 2004), pp. 159–171.
[31] H. Kuhn and C. Kuhn, Angew. Chem., Int. Ed. Engl. **42**, 262 (2003).
[32] N. Nandi, J. Phys. Chem. A **107**, 4588 (2003).
[33] N. Nandi, Curr. Sci. **88**, 1929 (2005).

[34] N. Nandi, J. Phys. Chem. B **108**, 789 (2004).
[35] M. A. Marahiel, T. Stachelhaus, and H. D. Mootz, Chem. Rev. **97**, 2651 (1997).
[36] H. von Döhren and U. Keller, J. Vater and R. Jocher, Chem. Rev. **97**, 2675 (1997).
[37] T. Stachelhaus and C. T. Walsh, Biochemistry **39**, 5775 (2000).
[38] G. L. Challis and J. H. Naismith, Curr. Opin. Struct. Biol. **14**, 748 (2004).
[39] G. Kreil, Annu. Rev. Biochem **66**, 337 (1997).
[40] N. Fuji, Orig. Life Evol. Biosph. **32**, 103 (2002).
[41] A. M. Torres, M. Tsampazi, E. C. Kennett, K. Belov, D. P. Geraghty, P. S. Bansal, P. F. Alewood, and P. W. Kuchel, Amino Acids **32**, 63 (2007).
[42] M. Friedman, J. Agric. Food Chem. **47**, 3457 (1999).
[43] E. Ohnishi, H. Macleod, and N. H. Horowitz, J. Biol. Chem. **237**, 138 (1962).
[44] W. S. Champney and R. A. Jensen, J. Bacteriol. **104**, 107 (1970).
[45] R. A. Jensen, S. L. Stenmark, and W. S. Champney, Arch. Mikrobiol. **87**, 173 (1972).
[46] S. D. Cosloy and E. McFall, J. Bacteriol. **114**, 685 (1973).
[47] J. Rytka, J. Bacteriol. **121**, 562 (1975).
[48] C. L. Harris, J. Bacteriol. **145**, 1031 (1981).
[49] T. Tsuruoka, A. Tamura, A. Miyata, T. Takei, K. Iwamatsu, S. Inouye, and M. Matsuhashi, J. Bacteriol. **160**, 889 (1984).
[50] M. Friedman, Adv. Exp. Med. Biol. **289**, 447 (1991).
[51] M. Caparros, J. L. M. Torrecuadrada, and M. A. de Pedro, Res. Microbiol. **142**, 345 (1991).
[52] M. Capparos, A. G. Pisabarro, and M. A. de Pedro, J. Bacteriol. **174**, 5549 (1992).
[53] J. Shoji and T. Kato, J. Antibiot. **29**, 1275 (1976).
[54] F. Peypoux, D. Marion, R. Maget-Dana, M. Ptak, B. Das, and G. Michel, Eur. J. Biochem. **153**, 335 (1985).
[55] K. Sivonen, M. Namikoshi, W. Evans, M. Fardig, W. Carmichael, and K. Rinehart, Chem. Res. Toxicol. **5**, 464 (1992).
[56] R. Jack and G. Jung, Chimia. **52**, 48 (1998).
[57] E. Man, G. Fisher, I. Payan, R. Cadilla-Perezrios, N. Garcia, R. Chemburkar, G. Arends, and W. Frey II, J. Neurochem. **48**, 510 (1987).
[58] G. Fisher, A. D. Aniello, A. Vetere, and G. Cusano, M. Chavez and L. Petrucelli, Neurosci. Lett. **143**, 215 (1992).
[59] M. Schell, O. Cooper, and S. Snyder, Proc. Natl. Acad. Sci. USA **94**, 2013 (1997).
[60] H. Wolosker, S. Blackshaw, and S. Snyder, Proc. Natl. Acad. Sci. USA **96**, 13409 (1999).
[61] H. Wolosker, K. Sheth, M. Takahashi, J. Mothet, R. Brady, C. Ferris Jr, and S. Snyder, Proc. Natl. Acad. Sci. USA **96**, 721 (1999).
[62] E. W. Miles, R. S. Phillips, H. J. C. Yeh, and L. A. Cohen, Biochemistry **25**, 4240 (1986).
[63] S. A. Ahmed, B. Martin, and E. W. Miles, Biochemistry **25**, 4233 (1986).
[64] J. Soutourina, S. Blanquet, and P. Plateau, J. Biol. Chem. **275**, 11626 (2000).
[65] H. Kumagai, N. Kashima, and H. Yamada, Biochem. Biophys. Res. Commmun. **39**, 796 (1970).
[66] D. E. Metzler, M. Ihawa, and E. E. Snell, J. Am. Chem. Soc. **76**, 648 (1954).
[67] J. Jacques, A. Collet, and S. H. Wilen, *Enantiomers, Racemates and Resolutions* (John Wiley, New York, NY, 1981).
[68] T. C. Bruice, Annu. Rev. Biochem. **45**, 331 (1976).
[69] J. F. Kirsch, G. Eichele, G. C. Ford, M. G. Vincent, J. N. Jansonius, H. Gehring, and P. Christen, J. Mol. Biol. **174**, 497 (1984).
[70] P. H. von Hippel and O. G. Berg, J. Biol. Chem. **264**, 675 (1989).
[71] S. Bachman, K. R. Knudsen, and K. A. Jørgensen, Org. Biomol. Chem. **2**, 2044 (2004).
[72] M. E. Tanner, Acc. Chem. Res. **35**, 237 (2002).
[73] A. S. Spirin, FEBS Letters **514**, 2 (2002).

[74] (a) N. Ban, P. Nissen, J. Hansen, P. B. Moore, and T. A. Steitz, Science **289**, 905 (2000); (b) P. Nissen, J. Hansen, N. Ban, P. B. Moore, and T. A. Steitz, Science **289**, 920 (2000).
[75] S. Pizzarello and A. L. Weber, Science **303**, 1151 (2004).
[76] J. C. Lacey Jr, N. S. M. D. Wickramasinghe, G. C. Cook, and G. Anderson, J. Mol. Evol. **37**, 233 (1993).
[77] (a) R. E. Monro and K. A. Marcker, J. Mol. Biol. **24**, 347 (1967); (b) R. E. Monro, J. Cerna, and K. A. Marcker, Proc. Natl. Acad. Sci. (USA) **61**, 1042 (1968).
[78] A. Bhuta, K. Quiggle, and T. Ott, D. Ringer and S. Chladek, Biochemistry **20**, 8 (1981).
[79] K. Quiggle, G. Kumar, T. W. Ott, E. K. Ryu, and S. Chladek, Biochemistry **20**, 3480 (1981).
[80] S. M. Hecht, Tetrahedron **33**, 1671 (1977).
[81] M. Sprinzl and F. Cramer, Prog. Nucleic Acid Res. Mol. Biol. **22**, 1 (1979).
[82] R. J. Harris and S. Pestka, in *Molecular Mechanisms of Protein Biosynthesis*, edited by H. Weissbach (Academic Press, New York, NY, 1977), pp. 413–422.
[83] R. Calendar and P. Berg, J. Mol. Biol. **26**, 39 (1967).
[84] T. Yamane, L. Miller, and J. J. Hopfield, Biochemistry **20**, 901 (1981).
[85] T. G. Heckler, Y. Zama, T. Naka, and S. Hecht, J. Biol. Chem. **258**, 4492 (1983).
[86] J. R. Roesser, M. S. Chorghade, and S. Hecht, Biochemistry **28**, 5185 (1989).
[87] T. G. Heckler, J. R. Roesser, C. Xu, P. I. Chang, and S. Hecht, Biochemistry **27**, 7254 (1988).
[88] J. R. Roesser, C. Xu, R. C. Payne, C. K. Surratt, and S. Hecht, Biochemistry **28**, 5185 (1989).
[89] J. D. Bain, E. S. Diala, C. G. Glabe, D. A. Wacker, M. H. Lyttle, T. A. Dix, and A. R. Chamberlin, Biochemistry **30**, 5411 (1991).
[90] S. Hecht, Acc. Chem. Res. **25**, 545 (1992).
[91] (a) D. Nathans, Proc. Natl. Acad. Sci. **51**, 585 (1964); (b) D. Nathans and A. Neidle, Nature (London) **197**, 1076 (1963).
[92] S. R. Starck, X. Qi, B. N. Olsen, and R. W. Roberts, J. Am. Chem. Soc. **125**, 8090 (2003).
[93] R. Zarivach, A. Bashan, R. Berisio, J. Harms, T. Auerbach, F. Schluenzen, H. Bartels, D. Baram, E. Pyetan, and A. Sittner, J. Phys. Org. Chem. **17**, 901 (2004).
[94] L. M. Dedkova, N. E. Fahmi, S. Y. Golovine, and S. M. Hecht, J. Am. Chem. Soc. **125**, 6616 (2003).
[95] L. Salem, X. Chapuisat, G. Segal, P. C. Hiberty, C. Minot, C. Leforestier, and P. Sautet, J. Am. Chem. Soc. **109**, 2887 (1987).
[96] K. Thirumoorthy and N. Nandi, J. Mol. Str. (THEO CHEM) **818**, 107 (2007).
[97] K. Thirumoorthy and N. Nandi, J. Phys. Chem. B **110**, 8840 (2006).
[98] (a) J. N. Israelachvili, *Intermolecular and Surface Forces* (Academic Press, London, 1985); (b) G. C. Maitland, M. Rigby, E. B. Smith, and W. A. Wakeham, *Intermolecular Forces: Their Origin and Determination* (Clarendon Press, Oxford, 1981).
[99] K. Thirumoorthy and N. Nandi, J. Phys. Chem. B **111**, 9999 (2007).
[100] J. L. Hansen, M. T. Schmeing, P. B. Moore, and T.A. Steitz, Proc. Natl. Acad. Sci. (USA) **99**, 11670 (2002).
[101] K. Thirumoorthy and N. Nandi, J. Phys. Chem. B **112**, 9187 (2008).
[102] S. I. Chamberlin, E. J. Merino, and K. M. Weeks, Proc. Natl. Acad. Sci. (USA) **99**, 14688 (2002).
[103] S. Dorner, N. Polacek, U. Schulmeister, C. Panuschka, and A. Barta, Biochem. Soc. Trans **30**, 1131 (2002).
[104] J. S. Weinger, K. M. Parnell, S. Dorner, R. Green, and S. Strobel, Nat. Struct. Mol. Biol. **11**, 1101 (2004).
[105] M. V. Rodnina, M. Beringer, and P. Bieling, Biochem. Soc. Trans. **33**, 493 (2005).
[106] J. S. Weinger and S. Strobel, Blood Cells Mol. Dis. **38**, 110 (2007).
[107] S. Trobro and J. Aqvist, Proc. Natl. Acad. Sci. (USA) **102**, 12395 (2005).

[108] T. M. Schmeing, K. S. Huang, D. E. Kitchen, S. A. Strobel, and T. A. Steitz, Mol. Cell. **20**, 437 (2005).
[109] A. Gindulyte, A. Bashan, I. Agmon, L. Massa, A. Yonath, and J. Karle, Proc. Natl. Acad. Sci. (USA) **103**, 13327 (2006).
[110] A. Sievers, M. Beringer, M. V. Rodnina, and R. Wolfenden, Proc. Natl. Acad. Sci. (USA) **101**, 7897 (2004).
[111] R. Schweet and E. Allen, J. Biol. Chem. **233**, 1104 (1958).
[112] M. V. Rodnina, M. Beringer, and W. Wintermeyer, Q. Rev. Biophys **39**, 203 (2006).
[113] P. K. Sharma, Y. Xiang, M. Kato, and A. Warshel, Biochemistry **44**, 11307 (2005).
[114] M. Ibba and D. Söll, Annu. Rev. Biochem. **69**, 617 (2000).
[115] J. M. Berg, J. L. Tymoczko, and L. Stryer, *Biochemistry* (W. H. Freeman & Co., New York, 2002), pp. 819–820.
[116] J. J. Hopfield, Proc. Natl. Acad. Sci. (USA) **74**, 2246 (1977).
[117] T. Yamane, L. Miller, and J. J. Hopfield, Proc. Natl. Acad. Sci. (USA) **71**, 4135 (1974).
[118] G. Archontis, T. Simonson, D. Moras, and M. Karplus, J. Mol. Biol. **275**, 823 (1998).
[119] A. R. Fersht, Biochemistry **26**, 8031 (1987).
[120] A. R. Fersht and C. Dingwall, Biochemistry **18**, 1245 (1979).
[121] A. R. Fersht, in *Accuracy in Molecular Processes*, edited by T. B. L. Kirkwood, R. F. Rosenberg, and D. J. Galas (Chapman & Hall, New York, NY, 1986), pp. 69–82.
[122] M. A. Rould, J. J. Perona, D. Söll, and T. A. Steitz, Science **246**, 1135 (1989).
[123] M. A. Rould, J. J. Perona, and T. A. Steitz, Nature **352**, 213 (1991).
[124] J. J. Perona, M. A. Rould, and T. A. Steitz, Biochemistry **32**, 8758 (1993).
[125] V. L. Rath, L. F. Silvian, B. Beijer, B. S. Sproat, and T. A. Steitz, Structure **6**, 439 (1998).
[126] K. J. Newberry, Y.-M. Hou, and J. J. Perona, EMBO J. **21**, 2778 (2002).
[127] E. Davie, V. Konigsberger, and F. Lipman, Arch. Biochem. Biophys. **65**, 21 (1956).
[128] R. Calendar and P. Berg, Biochemistry **5**, 1690 (1966).
[129] J. Soutourina, P. Plateau, and S. Blanquet, J. Biol. Chem. **275**, 32535 (2000).
[130] F. Bergmann, P. Berg, and M. Dieckmann, J. Biol. Chem. **236**, 1735 (1961).
[131] S. Norton, J. Ravel, C. Lee, and W. Shive, J. Biol Chem. **238**, 269 (1963).
[132] A. T. Profy and D. A. Usher, J. Mol. Evol. **20**, 147 (1984).
[133] K. Tamura and P. Schimmel, Science **305**, 1253 (2004).
[134] K. Tamura and P. Schimmel, Proc. Nat. Acad. Sci. (USA) **103**, 13750 (2006).
[135] D. Thompson, C. Lazennec, P. Plateau, and T. Simonson, J. Biol. Chem. **282**, 30856 (2007).
[136] S. Dutta Banik and N. Nandi, (submitted).
[137] J. G. Arnez, J. G. Augstine, D. Moras, and C. S. Francklyn, Proc. Natl. Acad. Sci. (USA) **94**, 7144 (1997).
[138] D. Tworowski, A. V. Feldman, and M. Safro, J. Mol. Biol. **350**, 866 (2005).
[139] E. J. Gabbay, Biochemistry **5**, 3036 (1966).
[140] E. J. Gabbay, Biopolymers **5**, 726 (1967).
[141] E. J. Gabbay and R. Kleinman, J. Am. Chem. Soc. **89**, 7123 (1967).
[142] E. J. Gabbay, K. Sanford, and C. Stuart Baxter, Biochemistry **11**, 3429 (1972).
[143] E. J. Gabbay, R. Kleinman, and R. R. Shimshak, J. Am. Chem. Soc. **90**, 1927 (1968).
[144] E. J. Gabbay, P. D. Adawadkar, and W. D. Wilson, Biochemistry **151**, 146 (1976).
[145] J. M. Alexander, J. L. Clark, T. J. Brett, and J. J. Stezowski, Proc. Natl. Acad. Sci. (USA) **99**, 5115 (2002).
[146] K. Ariga, T. Michinobu, T. Nakanishi, and J. P. Hill, Curr. Opin. Colloid Interface Sci. **13**, 23 (2008).
[147] K. Ariga, T. Nakanishi, and J. P. Hill, Soft Matter **2**, 465 (2006).
[148] T. Michinobu, S. Shinoda, T. Nakanishi, J. P. Hill, K. Fuji, T. N. Player, H. Tsukube, and K. Ariga, J. Am. Chem. Soc. **128**, 14478 (2006).
[149] J. Yuan and M. Liu, J. Am. Chem. Soc. **125**, 5051 (2003).

[150] K. Ariga, J. P. Hill, M. V. Lee, A. Vinu, R. Charvet, and S. Acharya, Sci. Technol. Adv. Mater. **9**, 014109 (2009).
[151] M. Khan, A. K. Sood, F. L. Deepak, and C. N. R. Rao, Nanotechnology **17**, S287 (2006).
[152] J. M. Thomas and R. Raja, Acc. Chem. Res. **41**, 708 (2008).
[153] T. Hermann, Curr. Opin. Struct. Biol. **15**, 355 (2005).
[154] N. Nandi, K. Bhattacharya, and B. Bagchi, Chem. Rev. **100**, 2013 (2000).